

We are IntechOpen, the world's leading publisher of Open Access books Built by scientists, for scientists

6,900

Open access books available

186,000

International authors and editors

200M

Downloads

Our authors are among the

154

Countries delivered to

TOP 1%

most cited scientists

12.2%

Contributors from top 500 universities



WEB OF SCIENCE™

Selection of our books indexed in the Book Citation Index
in Web of Science™ Core Collection (BKCI)

Interested in publishing with us?
Contact book.department@intechopen.com

Numbers displayed above are based on latest data collected.
For more information visit www.intechopen.com



Porous Structures in Heat Pipes

Patrik Nemec

Additional information is available at the end of the chapter

<http://dx.doi.org/10.5772/intechopen.71763>

Abstract

This work deals with heat pipes with porous wick structures and experiments depending on the wick structure porosity, because the porosity is one of the wick structure properties which has effect on the heat transport ability of the heat pipe. The work describes manufacturing porous wick structures for wick heat pipe by sintering of copper metal powders with various powder grain size; manufacturing porous wick structures for loop heat pipe by sintering of copper and nickel metal powders with various powder grain size; influence of manufacturing technology on the wick structure porosity by microscopic analysis of the porous structure; design and construction of wick heat pipe and loop heat pipes; experimental determination influence of the wick structure porosity on the heat transport ability of loop heat pipes at various conditions; and experimental and mathematical determination influence of the wick structure porosity on the heat transport ability of wick heat pipes at various conditions.

Keywords: wick heat pipe, loop heat pipe, wick structure, porosity, sintering, copper powder, nickel powder, heat transfer, thermal performance, mathematical calculation

1. Introduction

Two-phase heat transfer systems with capillary-driven offer important advantages over traditional single-phase systems. The most significant advantage associated with the phase change of a working fluid is higher heat transfer coefficient that results in enhanced heat transfer. Comparing with the single-phase liquid system, smaller mass flow rates are required to transport equivalent heat flux amounts for a given temperature range. Better thermal characteristics and lower mass flow rates offer the two-phase system benefit of smaller and lighter construction and increased performance. Single-phase system requires a high temperature gradient or a high mass flow rate to transfer high amount of heat flux, because thermal capacity of a single-phase system depends on the temperature change of the working fluid. The two-phase system provides essentially isothermal operation regardless of the heat load.

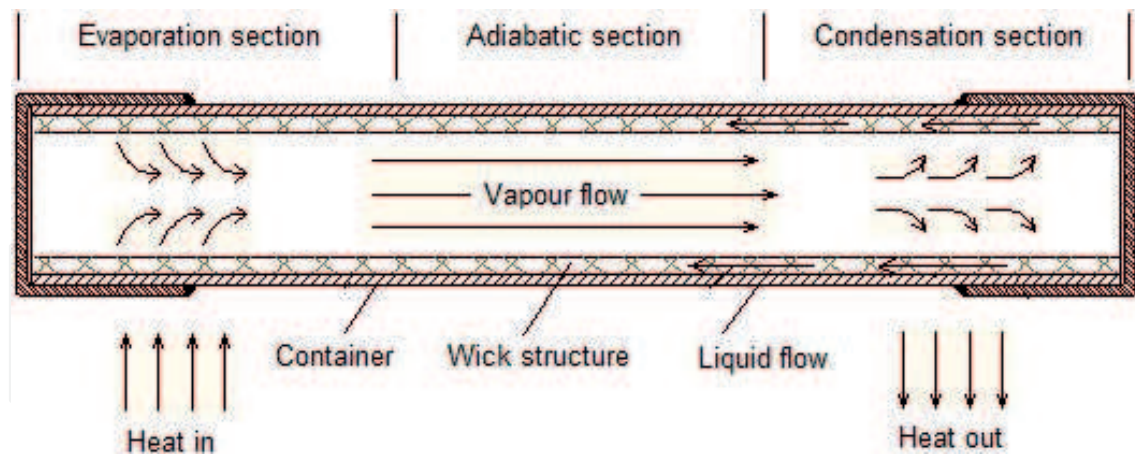


Figure 1. Schema of heat pipe.

Additionally, the single-phase systems need to working fluid circulation mechanical pumps or fans, while in the capillary-driven two-phase systems the working fluid circulate without any additional mechanical devices, which make such systems more reliable and free of electric power. The best known capillary-driven two-phase system is heat pipe and its schema is shown in **Figure 1**. The concept of the heat pipe was first suggested by Gaugler in 1944 [1] and by Trefethen [2] but was not widely publicized until serious development work by Grover and his co-worker in Los Alamos laboratory [3]. Heat pipes are passive heat transfer devices that transport heat from one point (heat source) to another (heat sink) with extremely high thermal conductance due the latent heat of vaporization of a working fluid. As shown in **Figure 1**, it consists of container, working fluid, wick structure and has three sections (an evaporator section, an adiabatic section, and a condenser section) [4].

Since one of the most important parts of the heat pipe HP and loop heat pipe LHP is the porous wick structure, this work is focused on experiments influencing porous wick structure on the heat transport ability of the heat pipe and loop heat pipe.

2. Heat pipe

The heat pipe is heat transfer device using the phase-change of working fluid to transfer heat from a heat source to heat sink and capillary forces generated in the wick structure to working fluid circulation. The heat pipe consists of hermetically closed container with wick structure on the inner surface and working fluid near its saturation temperature. Heat absorbed through the container to the liquid in the evaporator causes liquid evaporation and vapor flow through the open core of the heat pipe evaporator. The vapor flows out of the evaporator through the adiabatic section into the condenser. There the vapor condenses and released heat is transfer through wick structure and container wall into condenser ambient. Condensed liquid saturates the wick structure and creates capillary pressure; thus the liquid is pumped back into the evaporator. The operation of the heat pipe depends mainly on the parameters of container, working fluid and wick structure. Proper selection and design of the main heat pipe parts influence its operational characteristics defined by the heat transfer limitations, effective

thermal conductivity, and axial temperature difference. The two-phase heat transfer of the working fluid makes a heat pipe ideal for transferring heat over long distances with a very small temperature drop due to the temperature stabilization of the almost isothermal surface created during the operation. Almost isothermal condition of the heat pipe operation are related to working fluid operation in thermodynamic saturated state when the heat is transported using the latent heat of vaporization instead of sensible heat or conduction. Heat transported using the latent heat of vaporization is several times greater than heat transported by sensible heat for a geometrically equivalent system. The two-phase capillary-driven working fluid system allows efficiently to transfer large amounts of heat without additional mechanical pumping systems, decreasing the heat transfer area and thus saving the material, cost and weight. Wide range of the usable working fluid, high efficiencies, low dimensions and weights, and the absence of external pumps make heat pipes attractive options in a wide range of heat transfer applications [4].

2.1. Heat pipe construction

The heat pipe may have several basic parts depending on its type. During the heat pipe development, the main components and materials remained the same. The simplest type of heat pipe consists of two basic parts, the body (container) and the working medium. A capillary structure (wick) can be placed inside the heat pipe body to allow the condensed liquid phase of the working fluid wicking against the vapor flow due to the capillary action. Such a heat pipe is called a wick heat pipe. The heat pipe without capillary structure, is called gravitational heat pipe because it returns the liquid phase from the condenser part to the evaporator part which is due to gravity [5].

2.1.1. Container

The container of the heat pipe can have different shapes for different applications, but the most often is in the form of a closed pipe of a circular, flat or triangular cross-section. The main function of the heat pipe container is to isolate the working fluid from the outside environment. The container of the heat pipe should be strong enough to prevent internal dimension and internal pressure in case of compression or bending. The choice of the container material depends on many properties and should have the most appropriate combination (working fluid and environment compatibility, strength-to-weight ratio, thermal conductivity, porosity, wettability, machinability, formability, weldability or bondability). The container material should have a high thermal conductivity, solid and tough but easily machined, formable and easily soldered and welded. The surface of the material should be well-wetted, but at least as porous as possible to avoid gas diffusion. The materials of heat pipes are most commonly made of steel, copper, aluminum and their alloys. Various coatings of steel materials are also used [6].

2.1.2. Working fluid

Since the operation of the heat pipe is based on evaporation and condensation of the working fluid, its selection is an important factor in the design and manufacture of the heat pipe. The working fluid is chosen in particular according to the working temperature range of the heat pipe. Therefore, when selecting a working fluid, it is necessary to be careful if the operating temperature

range of the working fluid lies in the operating temperature range of the heat pipe. The heat pipe can operate at any temperature that is in the range between the triple and the critical point of the working fluid. The decision criterion at working fluid selection, in case of working fluids with the same operating temperature, is an appropriate combination of working fluid thermodynamics properties. The recommended features that working fluid should have are compatibility with the capillary structure material and the heat pipe container, good thermal stability, wettability of the capillary structure and heat pipe container, vapor pressure in the operating temperature range, high surface tension, low viscosity of the liquid and vapor phase, high thermal conductivity, high latent heat of vaporization, acceptable melting point and solidification point [6]. **Table 1** shows typical heat pipes working fluids sorted by operating temperature range.

2.1.3. Wick structures

The wick structure and working fluid generate the capillary forces that are required to pump liquid from the condenser to the evaporator and keep liquid evenly distributed in the wicking material. Heat pipe wicks can be classified as either homogeneous wicks or composite wicks. Homogeneous wicks are composed of a single material and configuration. The most common types of homogeneous wicks are wrapped screen, sintered metal and axial groove. Composite wicks are composed of two or more materials and configurations. The most common types of composite wicks are variable screen mesh, screen-covered groove, screen slab with grooves, and screen tunnel with grooves. Regardless of the wick configuration, the desired material properties and structural characteristics of heat pipe wick structures are a high thermal conductivity, high wick porosity, small capillary radius, and high wick permeability [6].

Working fluid	Melting point at atmospheric pressure (°C)	Boiling point at atmospheric pressure (°C)	Latent heat of vaporization (kJ kg ⁻¹)	Useful range (°C)
Helium	-271	-269	21	-271 to -269
Nitrogen	-210	-196	198	-203 to -160
Ammonia	-78	-33	1360	-60 to 100
Acetone	-95	57	518	0 to 120
Methanol	-98	64	1093	10 to 130
Ethanol	-112	78	850	0 to 130
Water	0	100	2260	30 to 200
Mercury	-39	361	298	250 to 650
Caesium	29	670	490	450 to 900
Potassium	62	774	1938	500 to 1000
Sodium	98	895	3913	600 to 1200
Lithium	179	1340	19,700	1000 to 1800
Silver	960	2212	2350	1800 to 2300

Table 1. Typical heat pipe working fluids.

2.2. Operation of heat pipe

In order of the heat pipe operation, the maximum capillary pressure must be greater than the total pressure drop in heat pipe.

Total pressure drop in heat pipe consist of three sections:

1. ΔP_l is pressure drop in the wick structure necessary to return the liquid from the condenser to the evaporator.
2. ΔP_v is pressure drop in the vapor core necessary to vapor flow from the evaporator to the condenser.
3. ΔP_g is pressure drop due gravity, depending on the heat pipe inclination that may be zero, positive or negative.

The correct operation of heat pipe must meet condition of:

$$\Delta P_{c, \max} \geq \Delta P_l + \Delta P_v + \Delta P_g \quad (1)$$

If heat pipe does not meet this condition, it will not operate due to the dry out of the wick in the evaporator section. This condition is referred as the capillary limit which determines the maximum heat flux of majority heat pipe operating range. The vapor velocity of liquid metal heat pipes may reach sonic values at start-up and with certain high-temperature. Then, heat pipe performance is limited by speed of sound, and compressibility effects must be taken into account in the calculation of the vapor pressure drop. Other most important limitations are the vapor pressure or viscous limit which occur at heat pipe stat-up when the heat pipe operates at low temperature. However the condenser pressure cannot be less than zero, the low vapor pressure of the liquid in the evaporator cause that the vapor pressure difference between evaporator and condenser of the heat pipe is insufficient to overcome viscous and gravitational forces. When the heat pipe operates at high heat fluxes, vapor flow may entrain liquid returning to the evaporator and cause dry out of the evaporator. This condition is referred as an entrainment limitation. Above mentioned limitations of the heat pipe relate to axial flow. During the heat pipe operation, temperature difference of radial heat flux is relatively small. When the heat flux reaches a critical value, the vapor blankets surface of evaporator wall results in an increase in temperature difference in evaporator. Limitation related to the radial flow of the heat pipe is referred as a boiling limit [7].

If stable liquid properties along the pipe, uniform wick structure along the pipe and neglect of pressure drop due to vapor flow are assumed, the total heat flux of heat pipe is given by

$$Q = \dot{m}_{\max} \cdot L. \quad (2)$$

$$\dot{m}_{\max} = \left[\frac{\rho_l \cdot \sigma_l}{\mu_l} \right] \cdot \left[\frac{K \cdot A}{l} \right] \cdot \left[\frac{2}{r_e} - \frac{\rho_l \cdot g \cdot l}{\sigma_l} \cdot \sin \theta \right] \quad (3)$$

3. Loop heat pipe

Loop heat pipe was developed to overcome the inherent problem of incorporating a long wick with small pore radius in conventional heat pipe by Gerasimov and Maydanik in 1972. LHP is a two-phase heat transfer device that utilizes the evaporation and condensation of a working fluid to remove heat and the capillary forces developed in fine porous wicks to circulate the fluid. **Figure 2** shows schema of LHP. It consists of an evaporator with wick structure, a compensation chamber, a condenser, and a liquid and vapor line. Wick structure is only in the evaporator and the compensation chamber. The rest parts of the LHP are made of smooth wall pipe. The wick structure of the evaporator has fine pores to create a capillary pressure and ensure working fluid circulation in the loop. The wick structure of the compensation chamber has larger pores for the purpose to transport working fluid to the evaporator. Heat applied to the evaporator causes that working fluid to start to evaporate and the vapor is pushed through the vapor line to the condenser due the capillary forces in the evaporator wick. Vapor condenses in the condenser and the liquid flows through the liquid line to the compensation chamber. The function of the compensation chamber is to store excess liquid and to control the operating temperature of the loop heat pipe. Thus, working fluid circulates without external pump in the loop [8, 9].

LHP can operate only if the capillary pressure developed in the evaporator wick is greater than the total pressure drop in the loop. The total pressure drop in the loop heat pipe is the sum of frictional pressure drops in the evaporator grooves, the vapor line, the condenser, the liquid line, the evaporator wick, and static pressure drop due to gravity:

$$\Delta P_{total} = \Delta P_{grove} + \Delta P_{vap} + \Delta P_{con} + \Delta P_{liq} + \Delta P_w + \Delta P_g \quad (4)$$

The capillary pressure of the evaporator wick is given by expression

$$\Delta P_{cap} = \frac{2\sigma \cdot \cos \theta}{R} \quad (5)$$

where, σ is the surface tension of the working fluid, θ is the contact angle between the liquid and the wick, and R is the radius of curvature of the meniscus in the wick. Increasing the heat load to the evaporator increases the mass flow rate and the total pressure drop in the system. The reaction to it, is the decrease of radius of curvature of the meniscus so that a capillary pressure will be higher than the pressure drop of total system. Increasing the heat load will decrease radius of curvature of the meniscus until the pore radius of the wick. The maximum capillary pumping capability of the wick is given by expression.

$$\Delta P_{cap, \max} = \frac{2\sigma \cdot \cos \theta}{R_v} \quad (6)$$

Further increase of the heat load will lead to vapor penetration through the wick and system deprime. Thus, under normal operation, the following condition must be satisfied at all times [10]:

$$\Delta P_{total} \leq \Delta P_{cap} \quad (7)$$

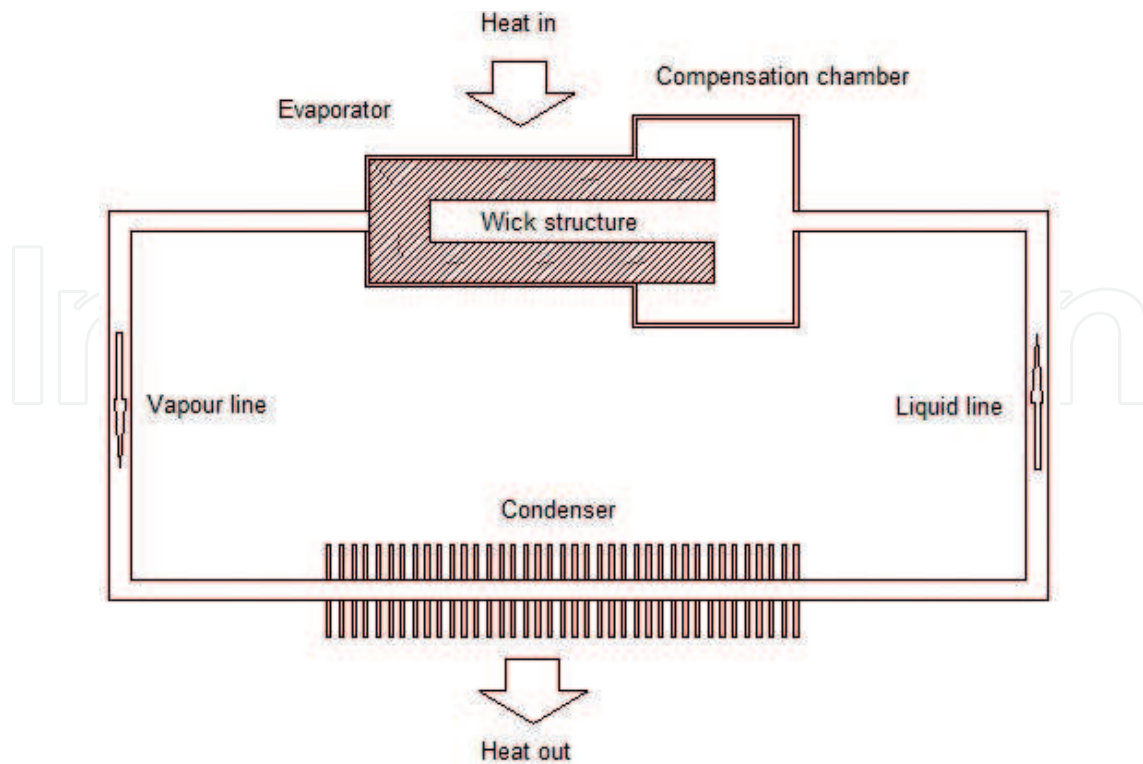


Figure 2. Schema of loop heat pipe.

Williams and Harris [11] investigated the in-plane and cross-plane properties of step-graded metal felt wicks for heat pipe applications. Porosity, effective pore radius, and liquid permeability were determined using imbibition, capillary flow porometry, and pressure-flow rate data, respectively. The authors determined that many of the correlations in the literature for pore size and permeability are too general in nature, echoing the conclusions of Bonnefoy and Ochterbeck [12] in regard to effective thermal conductivity.

Holley and Faghri [13] outlined methods for permeability and effective pore radius measurements based on the rate-of-rise test.

Typically, the rate-of-rise test requires observing the liquid front as it rises in a dry wick partially immersed in a liquid pool. As the precise location of this front can be difficult to detect, the authors devised a method using mass uptake rather than the meniscus front to determine the rate-of-rise of liquid in the wick. By analyzing the climbing meniscus, the authors developed a series of equations which could be used to numerically reduce the mass uptake data to yield permeability and pore size results.

Several relationships for permeability can be found, the most common is the Blake-Kozeny equation [14, 15], which gives the permeability of a bed of packed spheres as

$$K = \frac{r_p^2 \varepsilon^3}{37.5(1 - \varepsilon)^2} \quad (8)$$

where, K is permeability, r_p is pore radius, and ε is porosity.

Ren and Wu [16] modeled the effect of wick effective thermal conductivity in LHP evaporators; a two-dimensional axisymmetric model was developed yielding results in agreement with the literature in some respects, namely the position of the liquid front in relation to a heated fin [17, 18].

Zhao and Liao [18] presented temperature profiles indicating decreasing heat leak for increasing heat flux in a bed of packed spheres.

Iverson et al. [19] studied heat and mass transport in sintered copper wick structures. Wick samples were mounted vertically with the lower section immersed in a pool of water. A heater mounted to the back face of the wick applied power to the sample and the resulting temperature gradients were measured along with the mass flow rate of working fluid.

The majority of heat load is used in vaporization on the outer surface of wick [20]. The rest of heat input (called "heat leak") is conducted across the wick and is proportional to the effective thermal conductivity (ETC) of the capillary wicks [21]. Lower thermal conductivity of the porous wick ensures lesser heat conduction to the liquid inside the wick inner surface and maintains the operating temperature and thus the thermal resistance of the whole LHP.

Ku [10] and Furukawa [22] developed simplest LHP heat leak model that utilizes conductance parameter which varies with geometry and operating conditions.

$$Q_{e,cc} = G_{e,cc}(T_e - T_{cc}) \quad (9)$$

where Q is power, G is conductance parameter, and T is temperature of the evaporator and compensation chamber.

In steady state operation, the heat leak to the compensation chamber must be offset by the liquid returning from the condenser; Eq. (7) results, where ΔT represents the subcooling of the returning fluid

$$Q_{e,cc} = \dot{m}c_p\Delta T \quad (10)$$

where \dot{m} is mass flow and c_p is specific heat.

Chuang [23] developed a steady state LHP model which breaks the overall heat leak into two separate components: axially from the evaporator to the compensation chamber and radially from the heat source to the evaporator core. These two effects are related in that the formation of vapor bubbles in the evaporator core due to radial leak reduces the overall heat flow path back to the compensation chamber, increasing axial leak [10].

Chuang derived the following expressions for the axial and radial heat leak, respectively:

$$Q_{leak,a} = k_{eff}A\left(\frac{T_e - T_{cc}}{L}\right) + (Nuk_f\pi L)\left(\frac{T_e - T_{cc}}{2}\right) \quad (11)$$

$$Q_{leak,r} = \frac{2\pi k_{eff}L\zeta}{\left(\frac{r_o}{r_i}\right)^{\zeta-1}}\Delta T_W \quad (12)$$

where Q_{leak} is heat leak power, k_{eff} is effective thermal conductivity, A is area, L is characteristic length, Nu is Nusselt number, k_f is fluid thermal conductivity, and ζ represents a non-dimensional ratio of advection and conduction given by

$$\zeta = \frac{\dot{m}c_p}{2\pi k_{\text{eff}}L} \quad (13)$$

In his analysis and experiment, Chuang assumed this parameter to be zero, i.e., pure conduction. For the low power cases studied, this assumption was valid and resulted in low error; however, for high power levels or low wick conductivity, this assumption loses validity.

3.1. LHP wick structure

Wick structure is one of the main parts of loop heat pipe. To achieve good heat transfer ability of the LHP, wick structure with high porosity and permeability and fine pore radius is expected. The most frequently used wick structures in loop heat pipe are made of sintered metals, such as copper, nickel, stainless steel, titanium or polymers (polypropylene, polyethylene, PTFE) [24–26].

Reimbrechta et al. used a tap powder sintering technique by using a graphite matrix, to manufacture Ni wicks for capillary pump applications [27]. It shows that the graphite has low interaction with nickel by sintering the nickel powders at common sintering temperatures. Combination of two different methods, the cold-pressing sintering and the direct loose sintering, was used by Gongming et al. [28], for development of Ni and Ni-Cu (90% nickel and 10% copper) wicks for loop heat pipes. They found that using direct loose sintering technique with mean pore radii of 0.54 μm , an optimal Ni-Cu wick structure is prepared. Huang and Franchi [29] used copper screen mesh and two powder materials (nickel filamentary powder and spherical copper powder) to manufacture of bimodal wick structure. But it showed that these wicks may be produced with failures. Samanta et al. [30] developed metal injection molding Ni wick structures and performed study on its physical characteristic depending on sintering time (30, 60, and 90 min) and temperature (900, 930, and 950°C). Gernert et al. [31] developed fine pore wick structure for LPH. Wu et al. [32] discussed about the effect of sintering temperature curve in wick structure manufactured for LHP. Launay et al. referred a porosity, pore diameter, and permeability as the main parameters of wick structure in the work [20]. There is the optimal porosity of sintered wick referred between 30 and 75%, and the optimal permeability referred between 10^{-14} and $3 \times 10^{-13} \text{ m}^2$. The porosity of the wick structure decreases when the sintering temperature or the forming pressure increases. Majority of the sintered porous materials has pore diameters between 1 and 20 μm , except copper, which has pore diameters between 20 and 1000 μm .

In Ref. [33], the optimal capillary wick was found to be sintered at 650°C for 30 min, using direct loose sintering technique, with 90% nickel and 10% copper. The wick reaches the porosity of 70% and a mean pore diameter of 1.8 μm . In Ref. [10], biporous nickel wicks were fabricated. A porosity of 77.4% was achieved using cold pressure sintering method, at a temperature of 700°C, with a pore former content of 30% in volume.

4. Loop heat pipe experiments

The next experiment was performed in frame scientific research of porous structures suitable for LHP and finding possibility of heat removal produced by IGBT. The knowledge gained from the IGBT cooling by LHP has given us the information necessary to know how much heat flux LHP is able remove from heat source. This information will be in the future useful in the design of cooling devices working with the LHP.

4.1. Characterization of sintered structures

According to above-mentioned experiences with sintered structures for LHP, we decided to make wick structures from nickel and copper powder. At first, we do analysis of several sintered structures depending on grain size, sintering temperature, and sintering time on porosity, pore size, and strength. In an electric furnace, etalons were sintered from copper powders with grain sizes 50 and 100 μm and nickel powders with grain sizes 10 and 25 μm . The copper powders were sintered at temperature 800 and 950°C for time 30 and 90 min, and nickel powders were sintered at temperature 600°C for time 30 and 90 min.

4.1.1. Porosity measuring

The porosity of a wick structure describes the fraction of void space in the material, where the void may contain working fluid [34]. For the porosity measuring, the weight method was used. At first, the sample was weighed in dry state. Secondly, the sample was soaked with distilled water ($\rho = 0.998 \text{ g cm}^{-3}$ at 20°C). The weight of absorbed water was estimated by the difference between both values, and then a deduction of the “empty space” (thus the total pore volume) and the porosity.

$$\varepsilon = \frac{M_{ss} - M_{ds}}{V_{total} - \rho_w} \quad (14)$$

where ε is wick structure porosity, M_{ss} is weight of porous soaked sample, M_{ds} is weight of porous dry sample, V_{total} is pore volume of the porous sample, and ρ_w is density of absorbed liquid (water).

The results of porosity measuring are shown in **Tables 2–5**.

Grain size (μm)	50	50	50	50
Sintering temperature (°C)	800	800	950	950
Sintering time (min)	30	90	30	90
Porosity (%)	55	54	52	50

Table 2. Porosity of sintered structures from copper powder with grain size 50 μm .

Grain size (μm)	100	100	100	100
Sintering temperature ($^{\circ}\text{C}$)	800	800	950	950
Sintering time (min)	30	90	30	90
Porosity (%)	58	56	55	52

Table 3. Porosity of sintered structures from copper powder with grain size 100 μm .

Grain size (μm)	10	10
Sintering temperature ($^{\circ}\text{C}$)	600	600
Sintering time (min)	30	90
Porosity (%)	69	67

Table 4. Porosity of sintered structures from nickel powder with grain size 10 μm .

Grain size (μm)	25	25
Sintering temperature ($^{\circ}\text{C}$)	600	600
Sintering time (min)	30	90
Porosity (%)	72	70

Table 5. Porosity of sintered structures from nickel powder with grain size 25 μm .

4.1.2. Microscopic analysis of pore size

Investigation of etalons sintered structures by microscopic analysis shown, how influent is the sintering temperature and time on the pore size and on the ratio of the grain size to pore size of each structures. **Figures 3–8** of etalons were created by 100 time’s zoom of porous structures sintered from copper powder grain size 50 and 100 μm . **Figures 3** and **6** show that the structures sintered at temperature 800 $^{\circ}\text{C}$ have two times bigger pore than powder grain. Comparison of etalons sintered at temperatures 800 and 950 $^{\circ}\text{C}$ shows that the etalons sintered at temperature 800 $^{\circ}\text{C}$ have so much bigger pore size than at temperature 950 $^{\circ}\text{C}$. It means that pore sizes have so much width to create capillary action in structure. Comparison of etalons sintered at same temperature and various time intervals observed that the time of sintering at temperature nearest the melting temperature of sintering material is not decisive. Comparison of etalons at the same sintering temperature and time interval observed that the grain size of sintered material has impact on pore size. According to microscopic analysis of sintered structures, which clarifies their shape and profile, it can be concluded that the main influencing factors of pore size are grain size, sintering temperature, and not so much sintering time.

Next **Figures 9–12** were created by 500 times zoom of porous structures sintered from nickel powder grain size 10 and 25 μm . Comparison of etalons sintered from nickel powder led to the

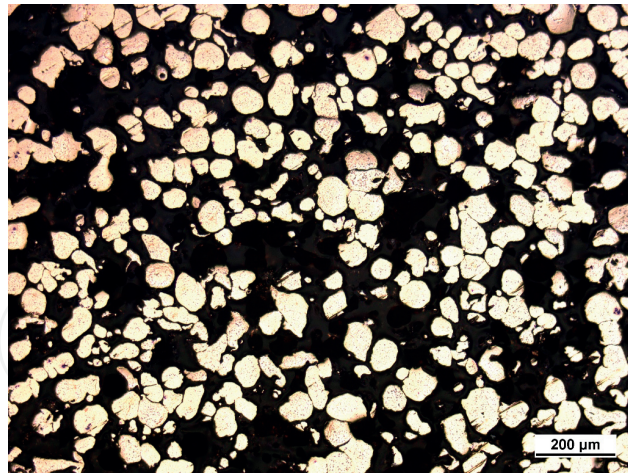


Figure 3. Grain size 50 μm, sintering temperature 800°C, sintering time 30 min.

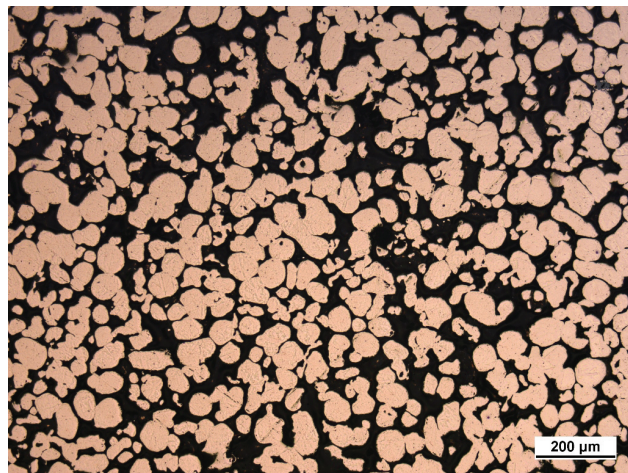


Figure 4. Grain size 50 μm, sintering temperature 950°C, sintering time 30 min.

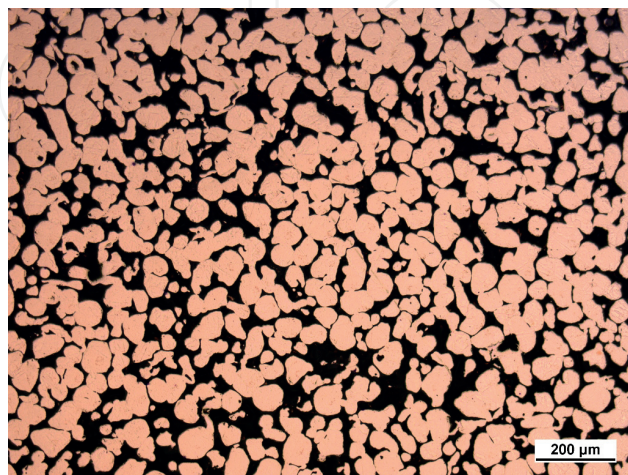


Figure 5. Grain size 50 μm, sintering temperature 950°C, sintering time 90 min.

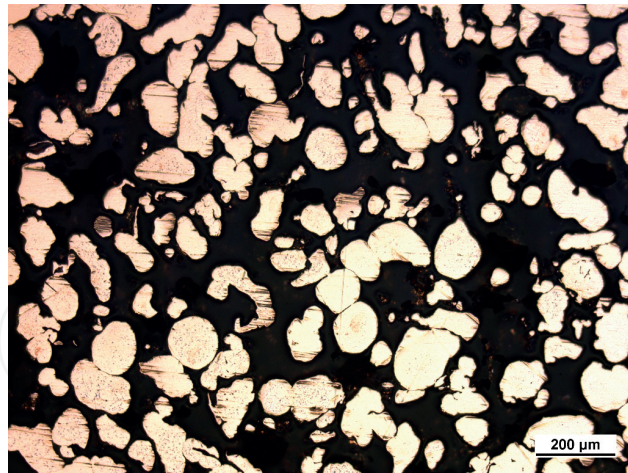


Figure 6. Grain size 100 μm , sintering temperature 800°C, sintering time 30 min.



Figure 7. Grain size 100 μm , sintering temperature 950°C, sintering time 30 min.

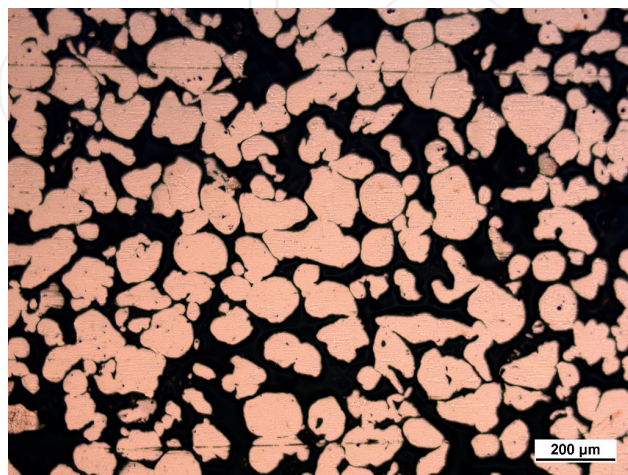


Figure 8. Grain size 100 μm , sintering temperature 950°C, sintering time 90 min.

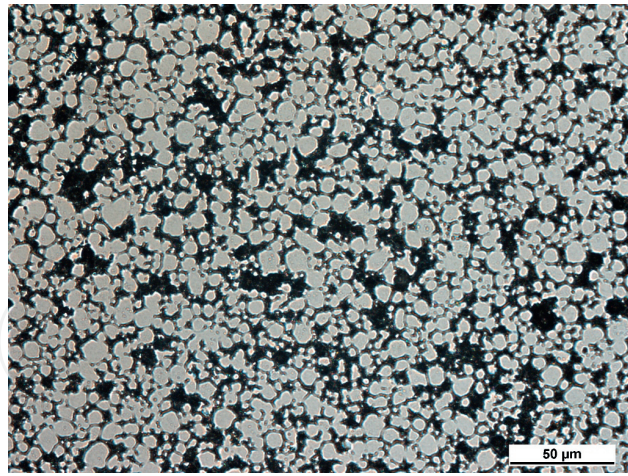


Figure 9. Grain size 10 μm, sintering temperature 600°C, sintering time 30 min.

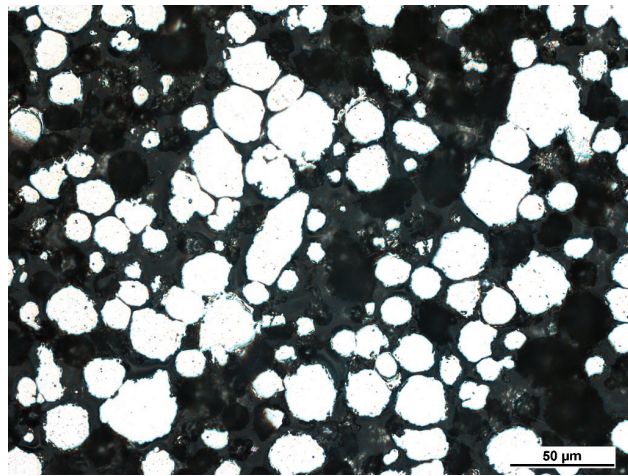


Figure 10. Grain size 25 μm, sintering temperature 600°C, sintering time 30 min.

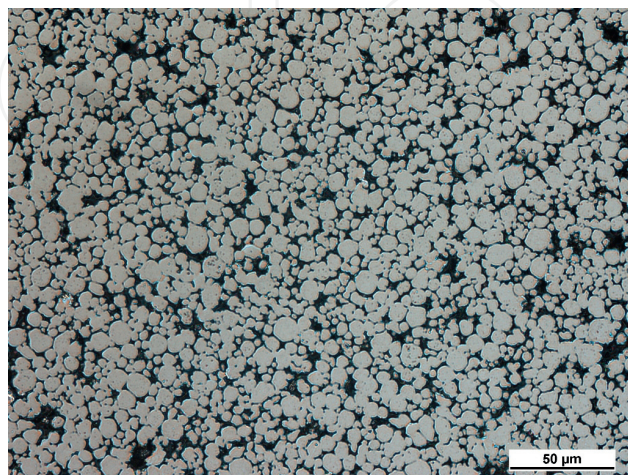


Figure 11. Grain size 10 μm, sintering temperature 600°C, sintering time 90 min.

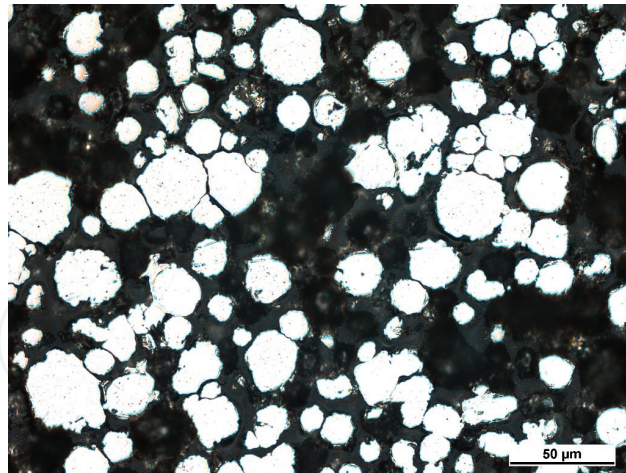


Figure 12. Grain size 25 μm , sintering temperature 600°C, sintering time 90 min.

same conclusion findings with etalons sintered copper powder. On the pore size, the formation of sintered structure does not affect sintering time but grain size.

4.2. Wick structure manufacture

From the results, porosity measurement and microscopic analysis were chosen for wick structure of LHP two copper etalons and two nickel etalons. The first structure was made of copper grain size 50 μm and sintered at temperature 950°C for 30 min (**Figure 13**). Second structure was made of copper grain size 100 μm and sintered at temperature 950°C for 30 min. Third structure was made of nickel grain size 10 μm and sintered at temperature 600°C for 90 min (**Figure 14**). The fourth structure was made of nickel grain size 25 μm and sintered at temperature 600°C for 90 min. The wick structures were sintered in send form (mold) and manufactured according to model of required shape in muffle furnace.

4.3. Loop heat pipe design

The experiments' goal was to determine the influence of various dependencies such as kind of wick structure, kind of working fluid, and amount of working fluid on LHP cooling efficiency. Therefore, special experimental LHP was designed with aluminum block mounted on the evaporator part to fix insulated gate bipolar transistor (IGBT). All parts of LHP (evaporator,



Figure 13. Porous sintered wick structures: a—Copper, b—Nickel.

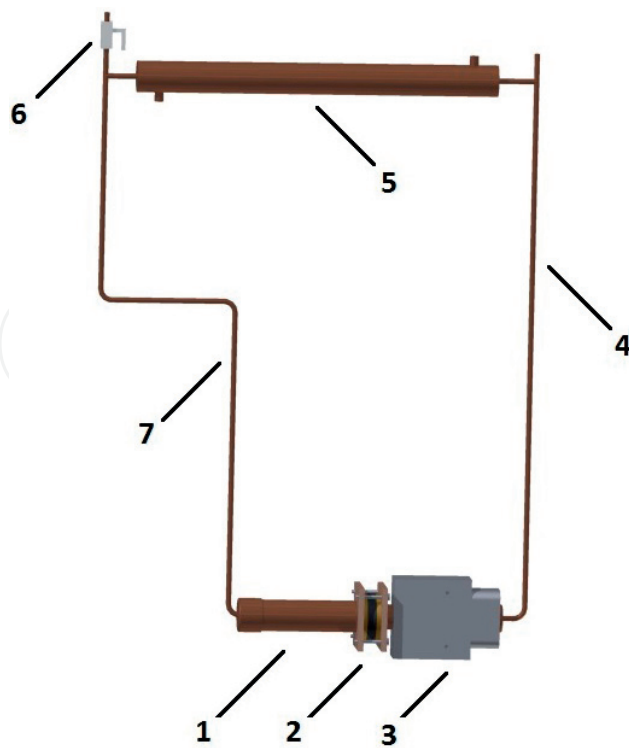


Figure 14. LHP model: 1—compensation chamber; 2—rubber seal; 3—evaporator; 4—vapor line; 5—condenser; 6—filling valve; 7—liquid line.

compensation chamber, vapor and liquid line) were made from copper pipes. As a working fluid, distilled water and acetone were used. Inside the evaporator, wick structure made by sintering metal powder was inserted. To avoid heat loss (it is also called heat leak) into the compensation chamber, a brass flange with rubber seal was inserted between the evaporator and the compensation chamber. In **Figure 15**, the model of LHP design is shown, and the main parameters of LHP design are given in **Table 6**.

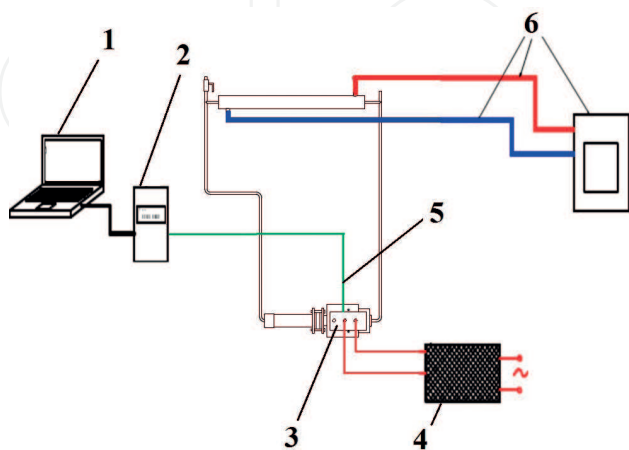


Figure 15. Schema of measuring unit: 1—PC; 2—data logger; 3—IGBT; 4—electric power supply; 5—thermocouple; 6—thermostat.

Evaporator		Compensation chamber	
Total length (mm)	130	Outer/inner diameter (mm)	35/33
Active length (mm)	86	Length (mm)	110
Outer/inner diameter (mm)	28/26	Charge mass	
Material	Copper	Distilled water	60%
Saddle		Vapor line	
Size (length/high/wide)	118/89/40	Length (mm)	670
Material	Alumina	Outer/inner diameter (mm)	6/4
Sintered copper powder		Liquid line	
Number of vapor grooves	6	Length (mm)	820
Porosity (%)	52–55	Outer/inner diameter (mm)	6/4
Outer/inner diameter (mm)	26/8	Condenser	
Sintered nickel powder		Length (mm)	420
Number of vapor grooves	6	Outer/ inner diameter (mm)	6/4
Porosity (%)	67–70		
Outer/inner diameter (mm)	26/8		

Table 6. Main design parameters of the LHP.

4.4. Determination of loop heat pipe cooling efficiency

Determination of the LHP cooling efficiency was performed on the experimental measuring unit, which is shown in **Figure 15**. Fixed IGBT on the evaporator of LHP was loaded by electric power. Produced heat by IGBT on the evaporator of LHP was removed by working fluid to the condenser of LHP. The condenser of LHP was made as tube heat exchanger and the cooling circle of heat exchanger was regulated by the thermostat at constant temperature 20°C. The gist of the LHP cooling efficiency determination is on measuring IGBT temperature with gradually increasing loaded heat by IGBT in steps 50 W from 100 W till the IGBT reaches permissible temperature 100°C. The temperature of the IGBT was measured by thermocouple inserted under IGBT. For better heat transport, thermal conductive paste was applied on the connection between IGBT and aluminum block and between aluminum block and the evaporator.

At first, measurements of influence of the working fluid amount on LHP cooling efficiency were performed. Four amounts 40, 50, 60, 80% of total LHP volume in LHP with working fluid water were investigated. In **Figure 16**, the influence of working fluid amount in dependencies on LHP cooling efficiency with working fluid water depending on loaded heat is shown. It is seen that the LHP with working fluid volume is 60% and the best operating LHP is in range of 150–350 W.

Next, the measurement of influence of wick structures on LHP ability to remove heat from IGBT was performed. The measurement was performed on LHP with the working fluid of water and amount of 60% total LHP volume. In **Figure 17**, the results of the influence of the wick structure on LHP cooling efficiency depending on loaded heat are shown. Two wick

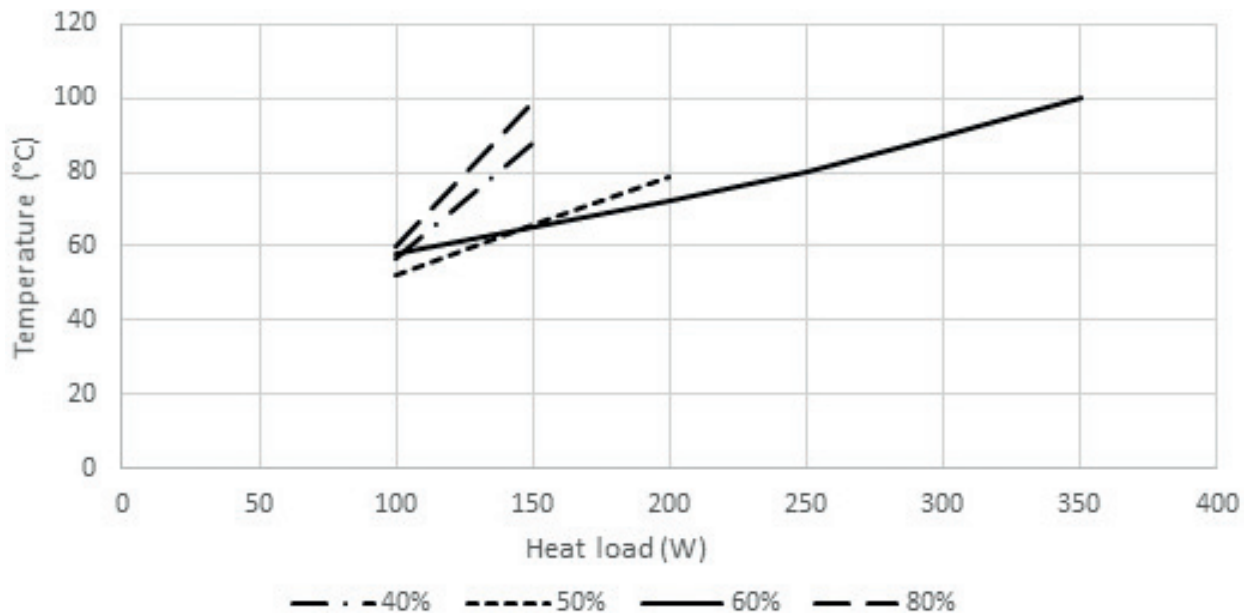


Figure 16. Influence of working fluid amount on LHP operation.

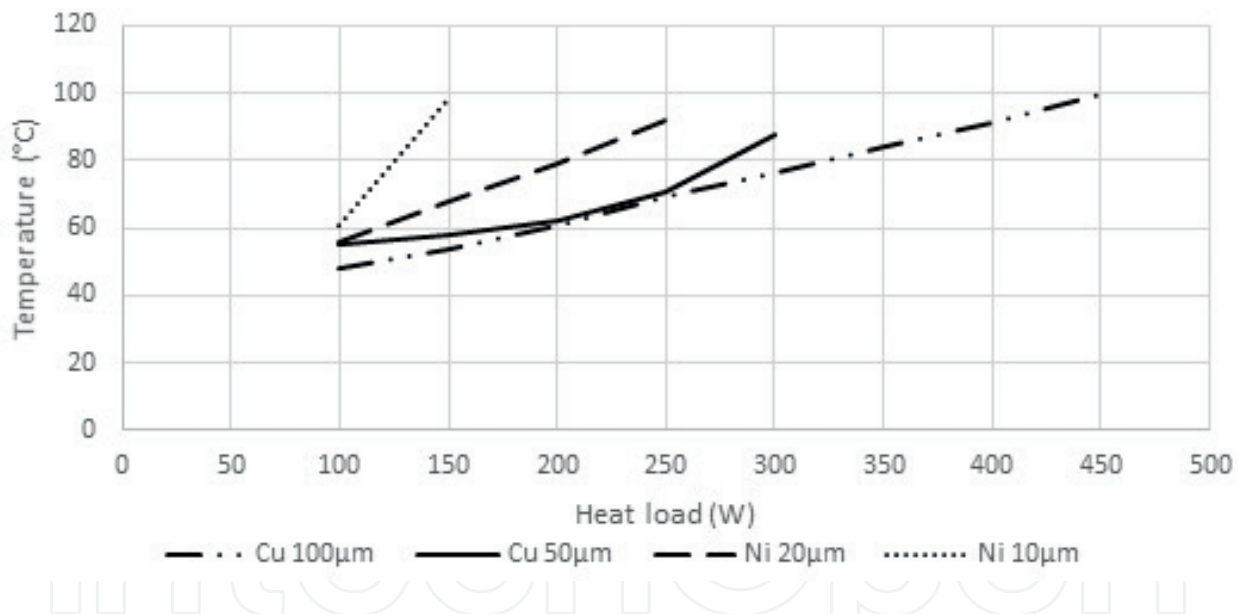


Figure 17. Influence of the wick structure on LHP cooling efficiency with working fluid water depending on loaded heat.

structures made from Cu powder with grain size 50 µm and 100 µm and two wick structures made from Ni powder grain size 20 µm and 10 µm were compared.

Comparing the results of dependence of temperature on input power of IGBT cooled by LHP with variants of sintered wick structure, the LHP with nickel wick structure does not show so good properties of heat removal than LHP with copper wick structure. Comparing the temperature curves of the LHP with first wick structure (made of Cu powder 50 µm) and LHP with second wick structure (made of Cu powder 100 µm), it is seen that both LHP have almost the same results at heat load of up to 200 W. At higher input power than 200 W loaded in to IGBT is

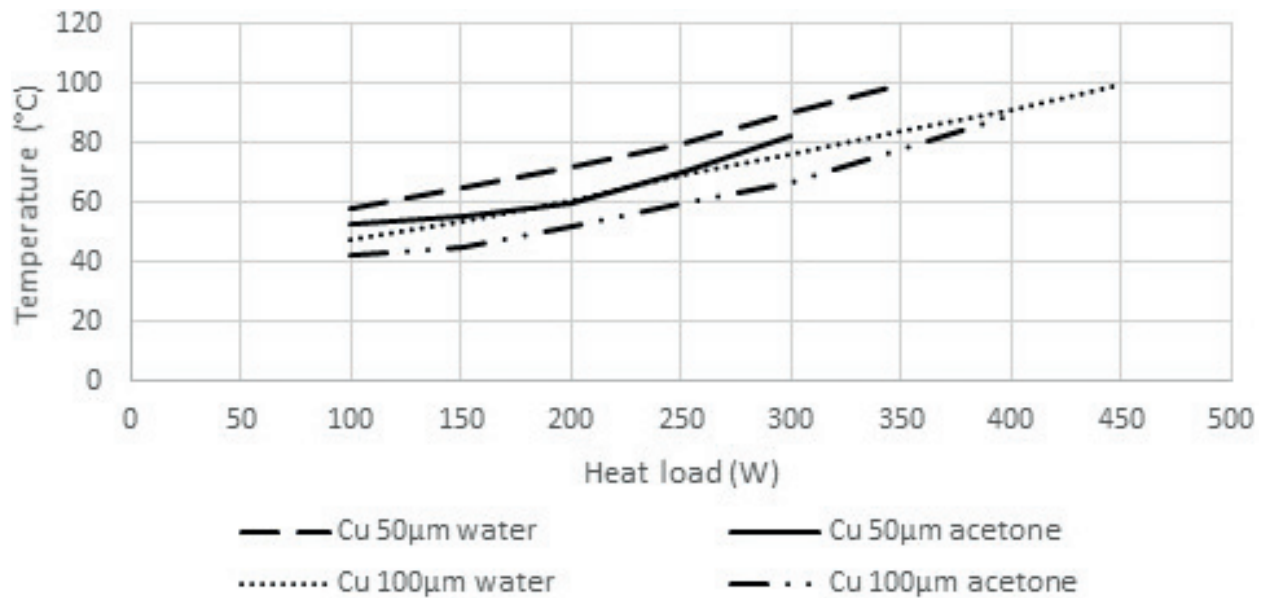


Figure 18. Influence of the working fluid on LHP cooling efficiency with wick structure made from Cu powder 100 µm and 50 µm depending on loaded heat.

seen that the LHP with first structure did not heat remove from IGBT and the temperature of IGBT exceed 100°C. The LHP with second wick structure is able to cool the IGBT under temperature 100°C until the IGBT input power 450 W. Comparing the temperature curves of the LHP with third wick structure (made of Ni powder 10 µm) and LHP with fourth wick structure (made of Ni powder 20 µm), it is seen that IGBT temperature cooled by LHP with third structure rapidly increases, already, at an input power 150 W. The LHP with fourth wick structure is able cool the IGBT under temperature 100°C until the IGBT input power 250 W.

At third, measurement impact of working fluid in LHP with wick structure made from Cu powder 100 µm and 50 µm and amount 60% of total LHP volume with an ability to remove heat from IGBT was performed. **Figure 18** shows the result of influence of the working fluid on LHP cooling efficiency depending on loaded heat. This experiment shows that the LHP with working fluid acetone better removes heat from the IGBT at lower heat load in range of 100–300 W. At higher heat loads is the better working LHP with the working fluid water.

5. Heat pipe experiments

The next experiments were performed in frame scientific research of porous wick heat pipes, where the ability of heat transfer depending on wick structure and working fluid is investigated. The popularity of porous wick heat pipe and lack of experiments performed with them were the reason to realize experiment which deals with heat pipes with sintered wick structures made from copper powders. This section describes manufacturing process of wick heat pipe, experimental measurement of heat transfer ability of heat pipe, and mathematical calculation of heat transport limitation of heat pipes.

5.1. Heat pipe manufacture processes

The main requirements on the heat pipe production are the high purity of the material of the individual parts and the working substance, as well as their mutual compatibility.

The basis of the heat pipe construction is the pipe body and the working fluid. The production of a heat pipe primarily consists in selecting a suitable material of the pipe and the working fluid. The working fluid is selected according to the temperature conditions in which the heat pipe will be used, because heat flux transferred by the heat pipe depends on the material of the pipe, the working fluid, and their mutual compatibility. An important part of the wick heat pipe is the wick structure, which also has a large impact on the amount of transferred heat flux.

The main components of heat pipe are:

- Pipe body (container)
- Working fluid
- Wick structure
- End caps
- Filling pipe

The heat pipe body may be of any cross-section, for example, circular or square, may include mounting flanges for ease of assembly, and may be bent into various shapes. The wick structure can be formed by grooves extruded into a pipe body or fine mesh screen, porous material and artery inserted into the heat pipe body [35]. In **Figure 19**, a schema of the wick heat pipe construction is shown.

The most common shape of the heat pipe is cylinder, because in addition of easily available product (wide assortment of material and the size of the pipe cross-sections), it provides certain advantages also in terms of strength and thermomechanical parameters. The advantage of producing a cylindrical shaped heat pipe is in the ease handling with the cylindrical material. In practice, heat pipes with a flat rectangular, triangular or other cross sections are also used. The most common heat pipes are manufactured with an inner diameter of 8–25 mm and an internal diameter of 2–5 mm—the so-called micro-heat pipes. The production process

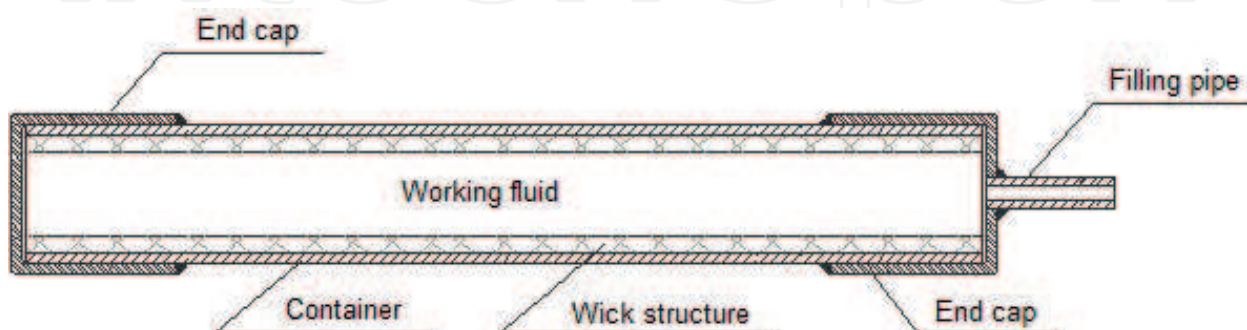


Figure 19. Schema of the wick heat pipe construction.

of the heat pipe can be divided into several sub-processes involving mechanical and chemical treatment of materials.

Technological process of the heat pipe production cycle:

- Body production and end caps.
- Production of wick structure.
- Cleaning of components.
- End caps closure by impervious joints (welding, soldering).
- Mechanical verification of body strength and tightness.
- Vacuuming of inner space and filling with the working fluid.
- Sealing the filling pipe (welding, soldering).

Before heat pipe production, it is necessary to thoroughly clean all components of the heat pipe to avoid any undesirable influence, which could ultimately have an effect on the heat transfer ability reduction. In cleaning process, first, mechanical impurities and rust from the body of the pipe are removed manually and then followed by chemical cleaning of the body, wick structure, end caps, and filling pipe [36].

5.1.1. Mechanical part of heat pipe manufacture

In the mechanical part of the production, the individual components of the heat pipe are first prepared: the body, the filling pipe, the wick structure, and the end caps. All components are then joined together by welding or soldering. In the case of wick heat pipe production, a wick structure is placed in the internal space of the body before to heat pipe closure. The closure of the heat pipe is the connection of the body with the end caps. In **Figure 20**, the standard types of the heat pipe closure by end caps are shown. The filling pipe is connected to one of the end caps due to the inner space vacuuming. After vacuuming, the heat pipe is filled with the working fluid,

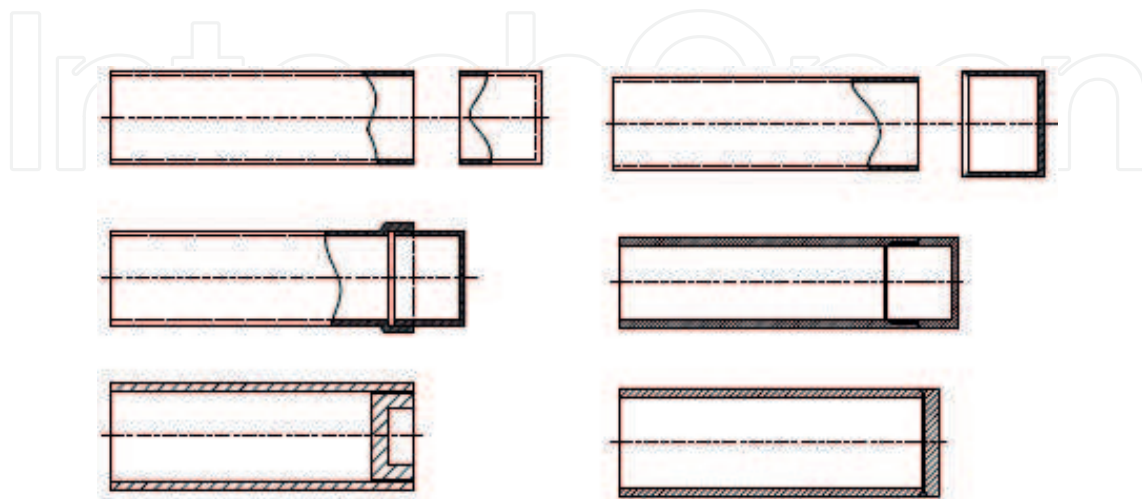


Figure 20. Types of the heat pipe closure by end caps.

filling pipe is pressed, and after disconnection from the vacuuming pump, filling pipe is sealed by soldering.

5.1.2. Chemical part of heat pipe manufacture

In the chemical part of the production, mechanical impurities and rust from the body of the heat pipe are first removed. This is followed by wet cleaning of the heat pipe components including cleaning with solutions, acids, and basic acids which are precisely determined for each type of material. The ultrasound cleaning, vacuuming, degassing, and passivation are processes that guarantee a high purity of the heat pipe material and thus contribute to long-lasting failure free operation. Generally, two important goals are achieved by cleaning. The first goal is to ensure good wetting material of the heat pipe well by working. The second goal is to remove all particles of dirt because the presence of impurities in solid, liquid or gaseous form may have an adverse effect on the heat transfer ability of heat pipe. Small particles can inhibit the formation of capillary pressure in the wick structure. Machining or human hand grease may reduce the wettability of the wick structure. Oxides formed on the walls of the wick structure may also reduce the ability of the working fluid to wet the surface. It is also highly advisable to use an ultrasonic cleaner to clean the heat pipe material, as the ultrasound breaks down impurities firmly absorbed on the surface of metallic particles that cannot be removed in any other way. The cleaning of the heat pipe is repeated immediately before filling with the working fluid, after connecting the body with the end caps and the filling tube. After cleaning, the tube is degassed by heating to a higher temperature and vacuuming the interior. In the case of a wick heat pipe, it is necessary to remove the oxide layers from the wick structure by chemical cleaning (e.g., solvents).

5.1.3. Filling the heat pipe with the working fluid

The working fluid added into the heat pipe must be completely clean, free from all mechanical impurities and gases, as their trace residues can also react with the body material of the heat pipe and the formation of undesirable elements. Clean substances can be purchased without any problems at special chemical stores. However, even in pure liquids and solids, an incompressible gas may be present. These gases can be removed by repeated freezing and thawing cycles. The working fluid in the filling bottle can freeze using the liquid nitrogen or dry ice.

Filling process of each type of working fluid is happening under other conditions. The characteristic of the filling process depends on the state of the working fluid at ambient temperature. If the working fluid is at the room temperature in the gaseous state (cryogenic), the filling can be carried out via a gas container of high quality. Filling and closing process of liquid-metal heat pipes is appropriate to do in the vacuum chamber [37].

The filling of low-temperature heat pipes can be carried out at room temperature without the use of any protective atmosphere. Before filling the heat pipe, it is advisable sucking the air from it to ensure the removal of undesirable components contained in the materials which could be later shown as non-condensing components. In addition, under pressure, the working fluid naturally enters into the heat pipe, and thus the equilibrium state of the pure vapor and liquid phases at a lower pressure than atmospheric will be achieved [38].

5.2. Heat pipe manufacture

Although the production of the porous wick structure is most difficult from all types of wick structures, it is one of the three most used wick structures in the heat pipe, because it is able to create a large capillary pressure that allows the heat pipe to transfer a high heat flux in the antigravity position. One method of making a porous wick structure is to sinter a copper powder uniformly poured around a coaxially centered steel mandrel located inside the copper pipe at a temperature close to melting the powder material in a high temperature electric furnace. By sintering copper powders is possible made wick structure with the high thermal conductivity, high wick porosity, small capillary radius, and high wick permeability what are the main which the wick structure have to ensure supplies evaporator with the condensed liquid. The high thermal conductivity of copper ensures that the wick structure will not have high thermal resistance, which is one of the expecting properties of wick structure too. The formation of a suitable porous structure by sintering the metallic powder depends, in addition to the sintering temperature, both on the time of sintering and the grain size of the powder. Copper powders with a particle size of 30–100 μm or copper fibbers of 2–3 mm in length and a diameter of 20–100 μm are used for the production of porous sintering structure.

The most important part of the heat pipe is wick structure. This experiment deal with heat pipes with sintered wick structure made from copper powder with granularity of 100, 63 and 35 μm by sintering in the high thermal electric oven using powder metallurgy. By sintering the copper powder on the inner wall of the heat pipe container, 1.5 mm thick wick structures were created. The sintering process of the wick structure was approx. at temperature of 1000°C and time of 30 min. Seeing that the pore size of the wick structure depends on the grain size of the copper powder, sintering the copper powder of various grain size creates the wick structure of various pore size. The overall length of the heat pipes is 0.5 m.

In **Figure 21**, copper powders are shown, and in **Figure 22**, manufactured porous wick structure are shown.

The other important part of the heat pipe design depends on factors related to the properties of the working fluid. The working fluid must have good thermal stability in relation to the specific working temperature and pressure. The most important requirements that the working fluid must have are the following: compatibility with the capillary system and with the material of the pipe, high thermal stability, high state of heat, high thermal conductivity, low

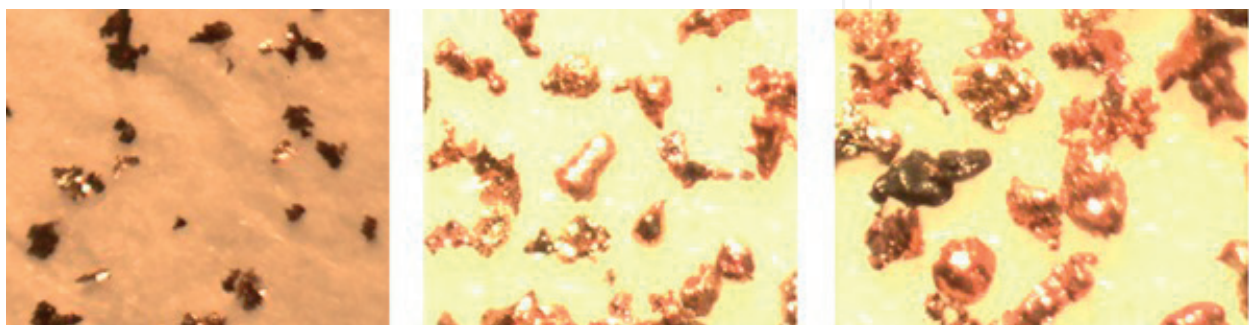


Figure 21. Copper powders (35, 63, and 100 μm).

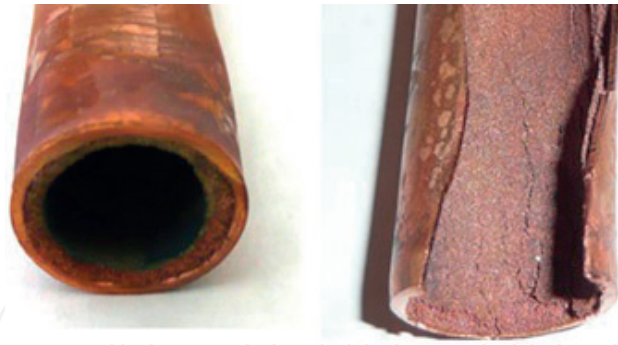


Figure 22. Sintered porous wick structures.

viscosity of the liquid and vapor phase, high surface tension, and acceptable freezing point. For this experiment, a working fluid water and ethanol were chosen.

The amount of the working fluid in heat pipes is other alchemy of the heat pipe manufacturing. There are some recommendations of working fluid amount in heat pipe. Lack of working fluid may lead to drying of evaporator part of heat pipe. Surplus working fluid can lead to congestion of the condensation part of the heat pipe. One of the recommendation about the working fluid amount in heat pipe is that the working fluid has to fill-up at least 50% of evaporator part of the heat pipe. In general, the quantity of the working fluid is determined in the range of 15–30% of the total heat pipe volume [35]. In this experiment, heat pipes was filled with working fluid of 20% total heat pipe volume.

And finally, the process of the vacuuming, filling and closing the heat pipe are the other important part of the heat pipe manufacture. There are some methods on how to perform this process. Each of these methods has a precise plan of filing and vacuuming processes. In **Figure 23**, schema of filling and vacuuming process used in heat pipe manufacturing is shown. Working fluid was injected into the pipe via connecting capillary tube by syringe. Heat pipe container with working fluid was connected to vacuum system and by vacuum pump, air from heat pipe container was sucked off. Before connecting pipe to vacuum system, the working fluid was cooled by the immersion of pipe into the cooling medium, because during

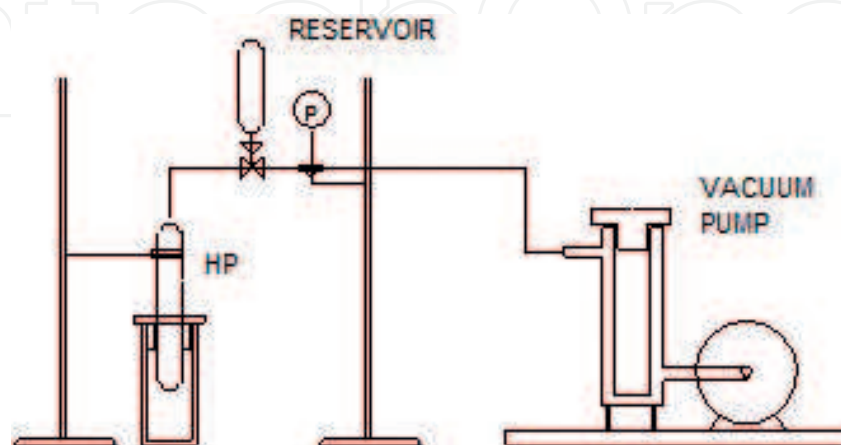


Figure 23. Schema of heat pipe filling and vacuuming process.

vacuuming of the pipe, pressure drop occurs and this may cause evaporation of working fluid. As a cooling medium, dry ice or liquid nitrogen may be used. After vacuuming, capillary tube connected was cramped, disconnected from vacuuming system and free-end soldered.

5.3. Heat transfer ability of the heat pipe

The main goal of the experiments is the determination of influence of the porous wick structure on the amount of thermal performance transferred by heat pipe. To determine the amount of thermal performance transferred by heat pipe, measuring unit consisting of measuring apparatus (thermostat, data logger, ultrasonic flowmeter, power supply) shown in **Figure 24** was proposed. Evaporator section of heat pipe was electrically heated by connecting to the laboratory power supply. Condensation section of heat pipe is placed into the heat exchanger where transferred heat from the evaporator is dissipated. Heat transferred by heat pipe is evaluated by calorimetric method emanating from calorimetric equation, where known mass flow, specific heat capacity, input and output temperature of cooling medium are flowing in the heat exchanger.

$$Q = \dot{m} \cdot c \cdot \Delta t \quad (15)$$

$$\Delta t = t_2 - t_1 \quad (16)$$

where Δt [°C]—temperature difference, t_1 [°C]—input temperature, t_2 [°C]—output temperature, \dot{m} [J kg⁻¹ K⁻¹]—mass flow of liquid, and c [J kg s⁻¹]—special thermal capacities of liquid.

In **Figure 25**, results of the experimental determination of influence of porous wick structure and working fluid on the heat pipe heat transfer ability at horizontal position and heat source 80°C are shown. It is seen that the heat pipe with working fluid water is able to transfer highest thermal performance in range 150–200 W. The best working wick structure in the water heat pipe is porous wick structure made from Cu powder with grain size 63 μm. On the other side, the porous wick structure made from Cu powder with grain size 35 μm is better for the heat pipes with working fluids such as acetone and ethanol that are able to transfer thermal performance

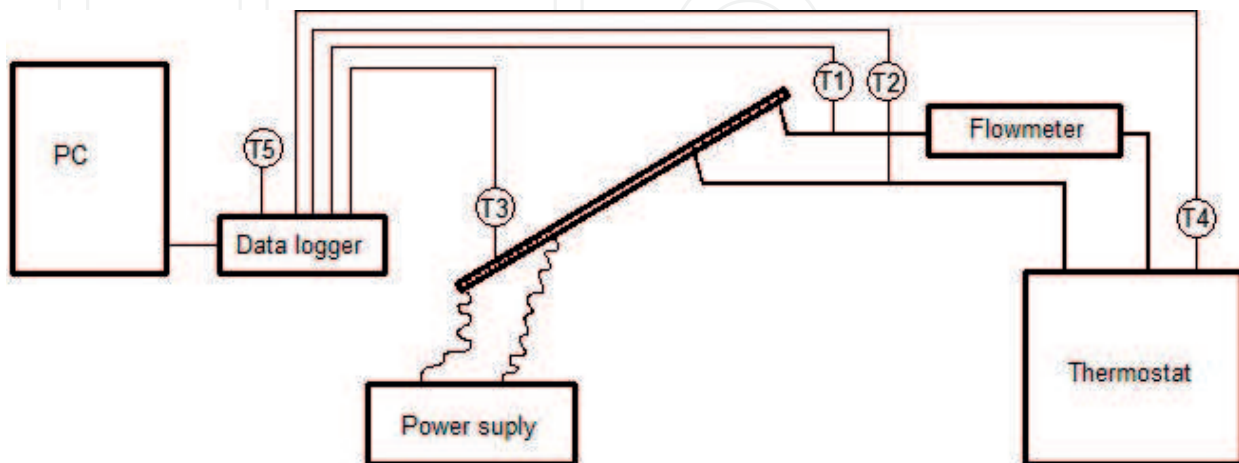


Figure 24. Scheme of measuring unit.

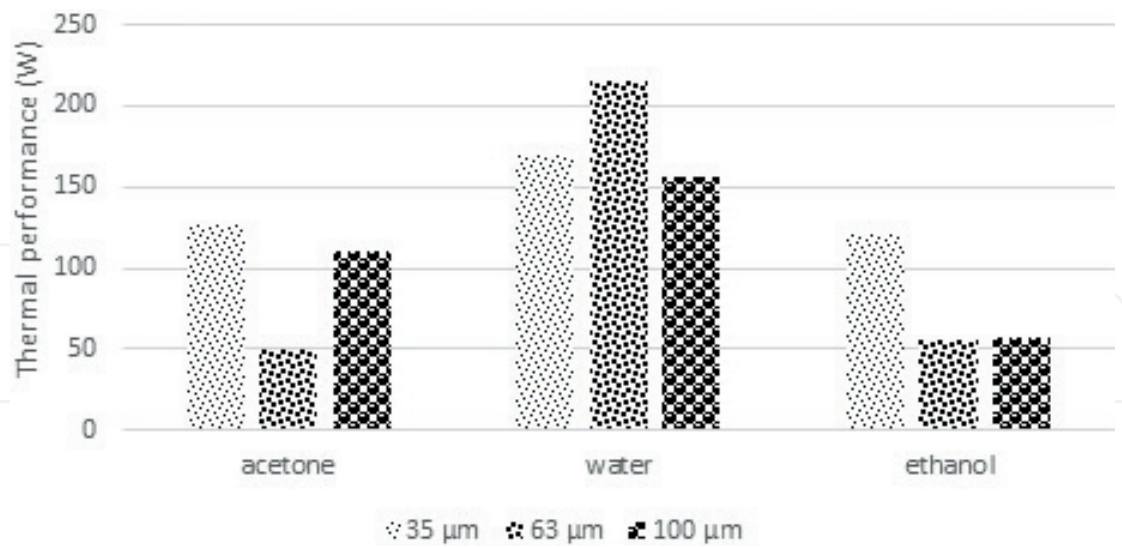


Figure 25. Influence of wick structure on the heat pipe heat transfer ability at heat source 80°C.

around 120 W. The experiment did not show the best one porous wick structure for selected working fluids, because each porous structure has various porosity and pore size which depend on the manufacturing process and each working fluid has different physical properties. There did not exist only one the best heat pipe with the best wick structure or the best working fluid because each heat pipe with various combination of the porous structure and working fluid is unique due its different properties.

In Figure 26, influence working position on the heat transfer ability of wick heat pipe with various porous wick structures is shown. Working position of heat pipe can divided into three

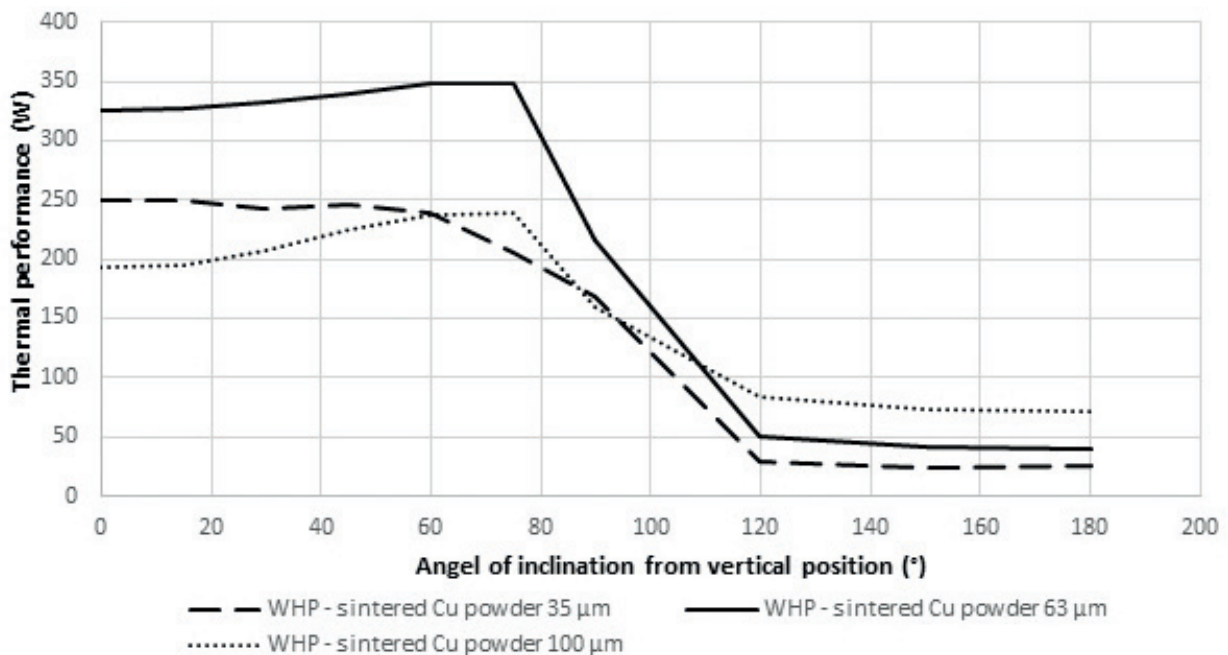


Figure 26. Dependence thermal performance on working position of wick heat pipes with various wick structures.

areas. Positive gravity action zone is represented by angle of inclination from vertical position $0\text{--}75^\circ$, zero gravity action zone (horizontal position) is represented by angle of inclination from vertical position 90° , and negative gravity action zone is represented by angle of inclination from vertical position $105\text{--}180^\circ$. There is seen that all wick heat pipe has good ability heat transfer in all zones. The best working wick heat pipe in positive and zero gravity action zone is heat pipe with wick structure made from Cu powder $63\ \mu\text{m}$. The best working heat pipe in zone with negative gravity action is wick heat pipe with wick structure made from Cu powder $100\ \mu\text{m}$.

5.4. Calculation of heat transfer limitation of the heat pipe

The heat flux transferred through the heat pipe depends mainly on the temperature difference and the corresponding thermal resistances. The real transferred heat is affected by the hydrodynamic and thermal processes that take place in the heat pipe at the various operating conditions. The heat flux transferred by the heat pipe can reach limit values that depend on these processes. There are five known limitations that limit the overall heat transfer in different parts of the heat pipe depending on the working temperature. In **Figure 27**, an ideal model of all heat transfer limitations that define area of maximum heat flux transferred by heat pipe depending on operating temperature is shown [4].

The mathematical model consists of calculation of the heat pipe heat transfer limitations. Heat pipe heat transfer limitations depend on the working fluid, the wick structure, the dimensions of the heat pipe, and the heat pipe operation temperature. Each heat transfer limitation expresses part of total heat flux heat pipe, which is influenced by hydrodynamic and thermal processes occurring in the heat pipe. Each of limitations exists alone and they are oneself non-influence together. To design mathematical model for the calculation of heat flux transferred by heat pipe,

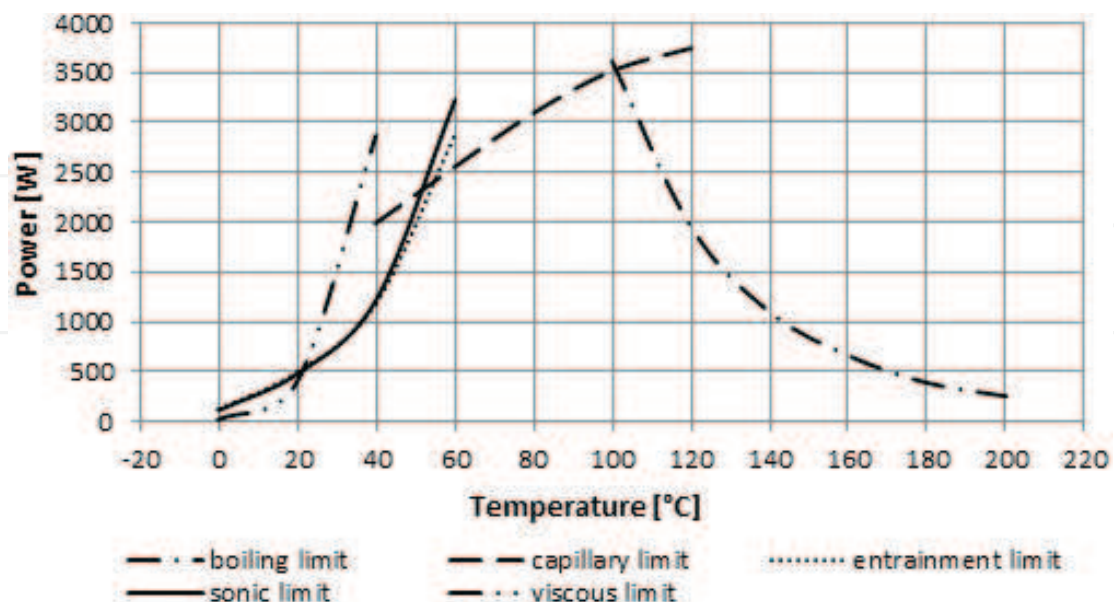


Figure 27. Heat transfer limitations of water wick heat pipe with sintered wick structure (heat pipe inner diameter 20 mm, total length 2 m, axial orientation 90° , sphere diameter of copper powder 0.85 mm, porosity 0.55, and width of wick structure 6 mm).

it is necessary to know basic and derived parameters of the heat pipe and its wick structure and physical properties of the working fluid liquid and vapor phase.

5.4.1. Capillary limitation

Capillary limitation involves a limitation that affects the wick heat pipe operation, which results from the capillary pressure acting on the condensed working fluid in the capillary structure. At the contact of liquid and wick structure surface, the capillary pressure is formed. This causes the liquid phase of the working fluid to flow from the condenser to the evaporator. Decreasing the pores of the capillary structure increases the capillary pressure as well as hydraulic resistance. The capillary limit occurs when the capillary forces at the interface of the liquid and vapor phases in the evaporator and condenser section of the heat pipe are not large enough to overcome the pressure losses generated by the friction. If the capillary pressure in the heat pipe during the operation is insufficient to provide the necessary condensate flow from the condenser to the evaporator, the capillary structure in the evaporator is dried and thus the further evaporation of the working substance is stopped. In general, the capillary limit is the primary limit that influences the heat pipe performance and is expressed by the relationship [39].

$$\dot{Q}_c = \frac{\sigma_l \cdot \rho_l \cdot l_v}{\mu_l} \cdot \frac{K \cdot A_w}{l_{eff}} \left(\frac{2}{r_{eff}} - \frac{\rho_l \cdot g \cdot l_t \cdot \cos \Psi}{\sigma_l} \right) \quad (17)$$

where A_w is the wick cross-sectional area (m^2), K is the wick permeability (m^2), μ_l is the liquid viscosity ($N \cdot s/m^2$), ρ_l is the liquid density (kg/m^3), g is the acceleration due to gravity (9.8 m/s^2), r_{eff} is the wick capillary radius in the evaporator (m), and l_t is the total length of the pipe (m) [7].

Furthermore, if the heat pipe has properly operated, the maximum capillary pressure has to be greater than the total pressure loss in the heat pipe and it is expressed by the relationship

$$(\Delta P_c)_{max} \geq \Delta P_{tot} \quad (18)$$

The maximum capillary pressure ΔP_c developed in wick structure of the heat pipe is defined by the Laplace-Young equation.

$$\Delta P_c = \frac{2\sigma}{r_{eff}} \cdot \cos \theta \quad (19)$$

where r_{eff} is the effective pores radius of the wick structure and θ is contact angle liquid phase of the working fluid in wick structure, where $\theta = 0^\circ$ is the best wetting contact angle [4].

5.4.2. Viscous limitation

When the heat pipe operates at low operating temperatures, the saturated vapor pressure may be very small and has the same range as the required pressure drop necessary for the vapor to flow from the evaporator to the condenser of the heat pipe. This results in a condition expressed by the viscous limit about balance of the vapor pressure and viscous forces in the

capillary structure in the low-velocity vapor flow. The most frequent cases of exceeding the boundary of the viscous limit occur when the heat pipe operates at temperature close to the solidification of the working fluid. In this case, working fluid evaporation in the evaporator and heat transfer in the form of vapor flow through the adiabatic section into the condenser of the heat pipe did not occur. It is assumed that the vapor is isothermal ideal gas, the water vapor pressure on the end of the condenser is equal to zero, which provides the absolute limit for the pressure in the condenser. The viscous limit is referred as the condition of the vapor phase flow at low velocity and is expressed by the relationship

$$Q_e = A_v \cdot l_v \cdot \left(\frac{\rho_v \cdot \sigma_l}{2 \cdot r_{c,ave}} \right)^{0.5} \quad (20)$$

where l_v is the latent heat of vaporization (J/kg), r_v is the cross-sectional radius of the vapor core (m), l_{eff} is the effective length of the heat pipe (m), μ_v is the vapor viscosity in the evaporator (N s/m²), P_v (Pa) is the vapor pressure, and ρ_v (kg/m³) is the density at the end of the heat pipe evaporator [4].

In cases when the viscous limit is reached for many conditions, the condenser pressure could not be a zero. Then the following expression is applied:

$$Q_b = \frac{4\pi l_{eff} \cdot \lambda_{eff} \cdot T_v \cdot \sigma_l}{l_v \cdot \rho_v \cdot \ln \frac{r_i}{r_v}} \cdot \left(\frac{1}{r_n} - \frac{1}{r_{eff}} \right) \quad (21)$$

where $P_{v,c}$ is the vapor pressure in the condenser [40].

5.4.3. Sonic limitation

The sonic limit characterizes the state in which the velocity of the evaporated vapor flow at the outlet of the evaporator reaches the sound velocity. Generally, this phenomenon occurs on the start of heat pipe operation at a low vapor pressure of the working fluid. Assuming that the vapor of the working fluid is the ideal gas and the vapor flow at the sound velocity throughout the heat pipe cross section is uniform, the sonic limit is determined by the relationship (22). The sonic limit does not depend on the heat pipe orientation and type of the heat pipe, and the same formula is applied for the gravity and wick heat pipe. The most difficult in the sonic limit determination is determining quantities of vapor density and pressure on inlet to the condenser [41].

$$Q_s = 0,474 \cdot A_v \cdot l_v \cdot (\rho_v \cdot P_v)^{0,5} \quad (22)$$

where ρ_v (kg/m³) is the vapor density, P_v (Pa) is pressure at the end of heat pipe evaporator, and A_v is the cross-sectional area of the vapor core (m²).

The sonic limit is mainly associated with liquid metal heat pipe startup or low-temperature heat pipe operation due to very low vapor densities that occur in these cases. For the low temperature or cryogenic temperatures, the sonic limit is not a typically factor, except for heat

pipes with very small vapor channel diameters. The sonic limitation is referred as an upper limit of the axial heat transport capacity and does not necessarily result in dry out of the wick structure in heat pipe evaporator or total heat pipe failure [4].

5.4.4. Entrainment limitation

Increasing the heat flux transferred by heat pipe increases the vapor flow velocity of the working fluid too and this results in a more pronounced interaction of the vapor and liquid phase inside the heat pipe. The interfacial surface becomes unstable and the viscous force on the surface of the liquid overcomes the forces of the surface tension. The waves are created on the liquid phase surface at first from which the droplets gradually tears off. At a certain vapor flow velocity, the liquid flow interruption into the evaporator section occurs. The condenser section of heat pipe is overfilled by vapor and liquid phase and the evaporator is overheated due to lack of the working fluid. The limit value of the heat flux, when the heat pipe condenser is overfilled by vapor and liquid, corresponds to interaction limit [42]. Entrainment limitation of the wick heat pipe is related to the condition when the vapor flows against the liquid flow in the wick structure, which may result in insufficient liquid flow in the wick structure [43]. Entrainment limitation of the wick heat pipe is expressed by relationship:

$$Q_e = A_v \cdot l_v \cdot \left(\frac{\rho_v \cdot \sigma_l}{2 \cdot r_{c,ave}} \right)^{0.5} \quad (23)$$

where $r_{c,ave}$ is the average capillary radius of the wick structure and, in many cases, it is approximated to r_{eff} and σ_l is the liquid surface tension (N/m) [4].

5.4.5. Boiling limitation

When heating the surface of the heat pipe wall with a layer of liquid in the saturation boundary, a three basic heat transfer regimes can occur. At low temperature difference of the heated surface and interfacial surface of the liquid, a natural convection and evaporation from the liquid surface occur. When increasing the temperature difference, a bubble boiling and gradual transformation to the film boiling occur. In heat pipe, a surface evaporation at low heat flux densities and bubble boiling at higher densities occur. Although the heat transfer intensity is greatest in the bubble boiling, for most types of wick heat pipes, the bubble boiling is not desired because it interferes with the liquid wicking into the wick structure. On the other hand, in a heat pipe with a grooved capillary structure, a gravity heat pipe with bubble boiling is favorable [44]. The heat flux in which the bubble boiling occurs in the wick heat pipes and the film boiling occurs in the gravity heat pipe is referred as the boiling limit. The gravity heat pipe is expressed by the relationship [45]:

$$Q_b = 0,16 \cdot A_v \cdot l_v \cdot \sqrt[4]{\sigma_l \cdot g \cdot \rho_v^2 (\rho_l - \rho_v)} \quad (24)$$

Determination of the boiling limit of the wick heat pipe is problematic, because it depends on a number of technological and operating conditions. The most reliable determination of the boiling limit is experimental determination for the particular wick structure and working fluid.

Approximate determination of the boiling limitation for the wick heat pipe is expressed by the relationship [46]

$$Q_b = 0,16 \cdot A_v \cdot l_v^4 \sqrt{\sigma_l \cdot g \cdot \rho_v^2 (\rho_l - \rho_v)} \quad (25)$$

where λ_{eff} is the effective thermal conductivity of the wick structure which is composed of the wick thermal conductivity and working fluid thermal conductivity (W/m K), T_v is temperature of vapor saturation (K), r_v is the vapor core radius, r_i is the inner container radius (m), and r_n is the bubble nucleation radius in range from 0.1 to 25.0 μm for conventional metallic heat pipe container materials [4].

5.4.6. Heat pipe parameters

To calculate heat pipe heat transport limitations, it is necessary to know thermophysical properties of working fluid in heat pipe, basic heat pipe parameters, thermal conductivity of heat pipe material, working temperature of heat pipe, axial orientation of heat pipe, and other heat pipe parameters calculated from basic heat pipe parameters.

$$l_t = l_e + l_{ad} + l_c \quad (26)$$

$$l_{\text{eff}} = 0.5(l_e + l_c) + l_{ad} \quad (27)$$

$$A_v = \pi r_v^2 \quad (28)$$

$$A_w = \pi (r_i^2 - (r_i - h)^2) \quad (29)$$

where l_t is total length of heat pipe [m], l_e is evaporation length of heat pipe [m], l_{ad} adiabatic length of heat pipe [m], l_c is condensation length of heat pipe [m], l_{eff} is effective length of heat pipe [m], A_v is cross-sectional area of the vapor core [m^2], A_w is wick cross-sectional area [m^2], r_v is cross-sectional radius of vapor core [m], r_i is inner container radius [m], and h is wick structure width [m].

The other parameters needed to calculate heat pipe heat transport limitations are basic parameters of sintered wick structure and other parameters calculated from basic parameters of wick structure.

$$r_{\text{eff}} = 0.21 \cdot d_s \quad (30)$$

$$K = \frac{d^2 \cdot \varepsilon^3}{150 \cdot (1 - \varepsilon)^2} \quad (31)$$

$$\lambda_{\text{eff}} = \lambda_l \frac{2 \cdot \lambda_l + \lambda_m - 2 \cdot (1 - \varepsilon) \cdot (\lambda_l - \lambda_m)}{2 \cdot \lambda_l + \lambda_m + (1 - \varepsilon) \cdot (\lambda_l - \lambda_m)} \quad (32)$$

where K is permeability [m^2], d is sphere diameter [m], ε is porosity [-], r_{eff} is effective radius of wick structure [m], λ_{eff} is effective thermal conductivity, λ_l is thermal conductivity of working fluid liquid, and λ_m is thermal conductivity of wick material [47].

5.5. Verification of mathematical model

The mathematical model was created according to above equations of limitations and input heat pipe parameters. Result of mathematical model is graphic dependencies of heat transport limitations on heat pipe working temperature. Mathematical model results of heat transport limitations of specific types of heat pipes were compare with results from measurement of heat pipe performance at temperatures 50°C and 70°C. In **Figure 28**, graphic comparison results of heat transport limitations determining total performance of heat pipe from mathematical model with measured performance of ethanol wick heat pipe with sintered wick structure and sphere diameter of copper powder 0.1 mm are shown. Dotted line creates boundary of heat pipe performance by capillary limitation and dashed line is boiling limitation. The full line is measured results of heat pipe thermal performance at temperature 50°C and 70°C. **Figure 29**

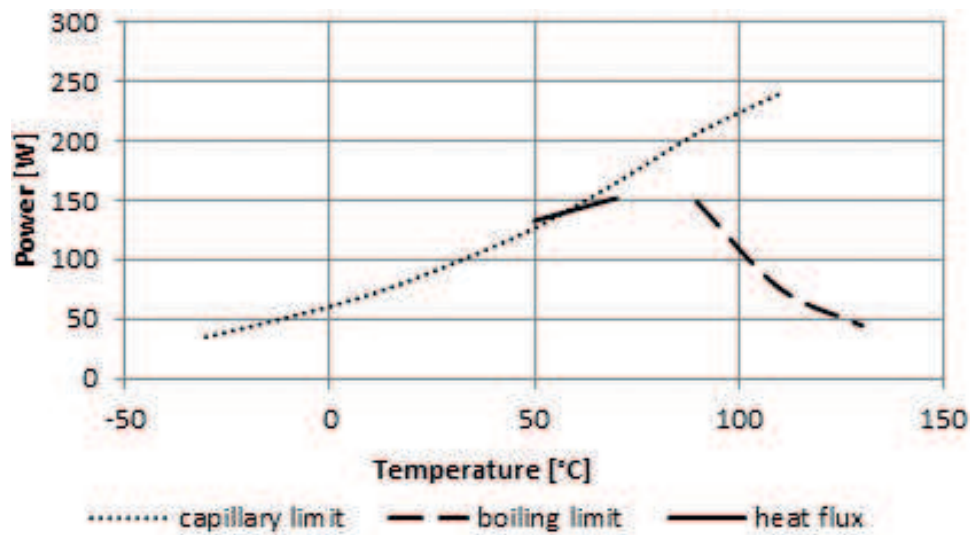


Figure 28. Verification of mathematical model by measuring of heat pipe performance (ethanol wick heat pipe with sintered wick structure and sphere diameter of copper powder 0.1 mm and axial orientation of heat pipe ψ 180°).

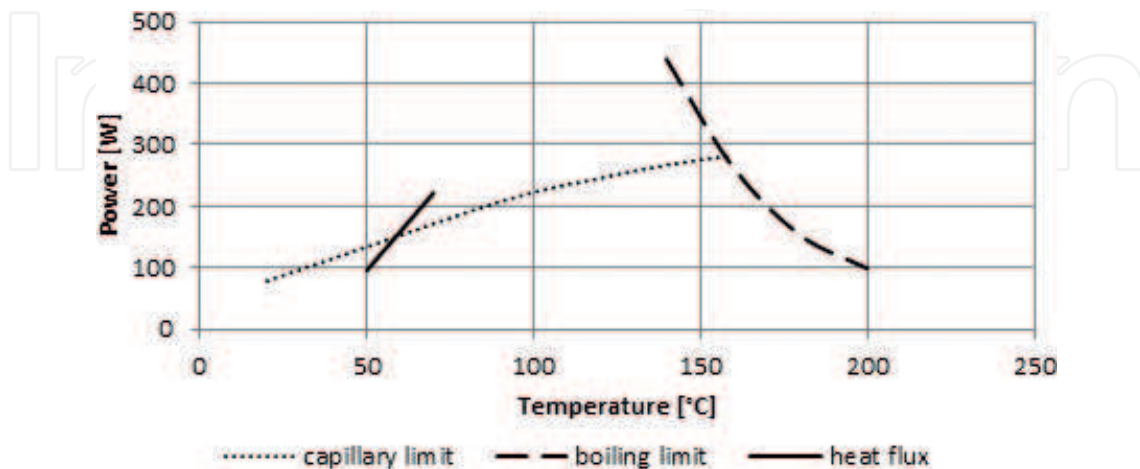


Figure 29. Verification of mathematical model by measuring of heat pipe performance (water wick heat pipe with sintered wick structure and sphere diameter of copper powder 0.63 mm axial orientation of heat pipe ψ 180°).

confirms the verification of mathematical model, where it is seen that the measured values of the transferred heat flux by heat pipe with sintered wick structure at temperatures 50°C and 70°C, are in approximately the same area as a calculated values of capillary limitation by mathematical model. In **Figures 28** and **29**, it is seen that the dotted line and full line are approximately in the same region at temperatures 50°C and 70°C.

5.6. Results of the mathematical model

Results of the heat pipe calculation are some interesting graphs of the maximal heat flux transferred by heat pipe depending on the wick structure parameters. It could be used in design optimization of the heat pipe wick structure. The curves present an area of maximal heat flux transferred by heat pipe depending on operating temperature.

Next graphic dependencies of heat pipe performance are created from mathematical model for ethanol wick heat pipe with sintered wick structure and various porosity, sphere diameter of copper powder, and wick structure width. In **Figure 30**, the influence of porosity on heat pipe performance is shown. Porosity of wick structure can change by adding some additives to sintered technology. There is clearly seen a rise in heat pipe performance with increasing porosity of wick structure. Heat pipe with the higher permeability of the wick structure can transfer higher heat flux. But with increasing permeability of wick structure, entrainment of liquid flow to evaporator by vapor flow can occur. This may cause dry out of heat pipe evaporation section and decrease total heat pipe performance.

In **Figure 31**, the influence of sphere diameter copper powder on sintered wick structure is shown. Using the bigger sphere diameter of copper powder to sintered technology, higher porosity wick structure is created. It can be said that increasing porosity is directly proportional to sphere dimension of copper powder, and to make more porosity wick structures, adding additives to sintered technology is not needed. In this case, an increase of heat pipe performance with used bigger sphere dimension of copper powder is seen.

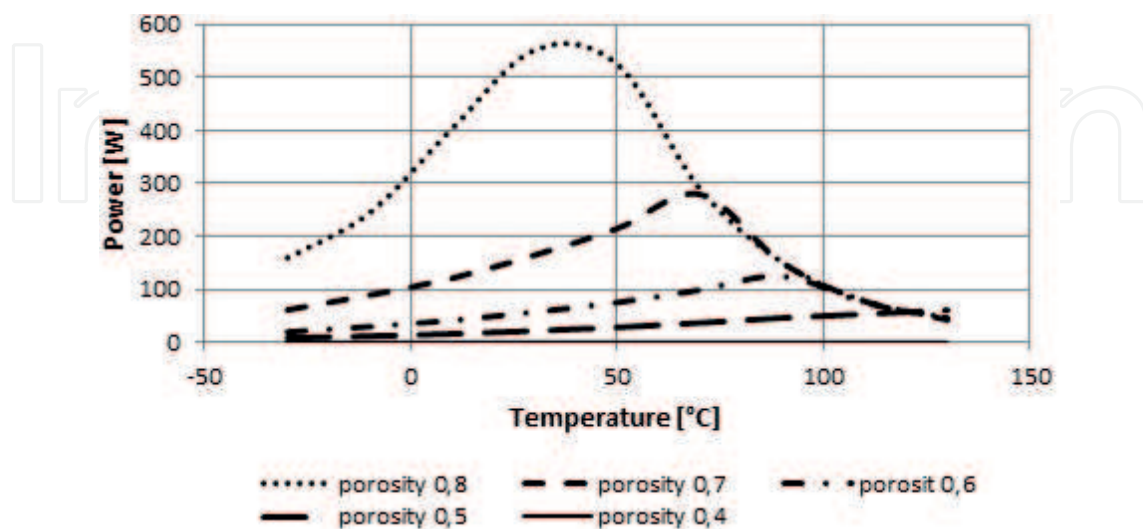


Figure 30. Dependence of heat pipe performance from wick structure porosity of the sintered wick heat pipe.

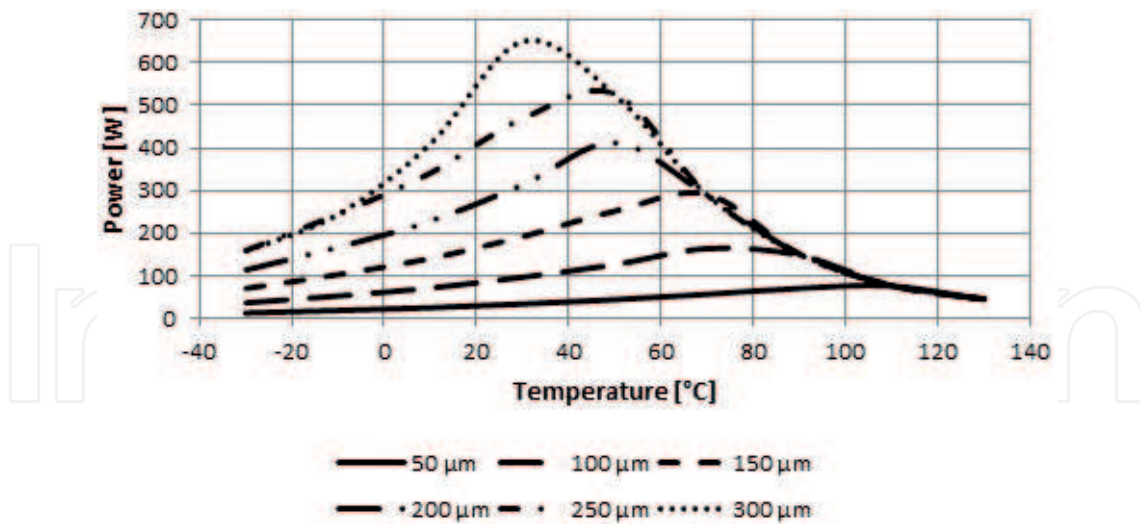


Figure 31. Dependence of heat pipe performance from sphere diameter of the copper powder in sintered wick heat pipe.

In Figure 32, the influence of wick structure width on heat pipe performance is shown. Wick structure width is an important factor, which influences heat pipe performance. It is seen that the heat pipe performance increases with the wick structure thickness in operating temperature region of -30 to 60°C . The capillary limitation is a main limitation for this region. On the other way, an increase of the wick structure thickness decreases the heat pipe performance in the operating temperature region of 80 – 130°C . It may be caused by bubble nucleation in wick structure, when the returning liquid from the condenser section to evaporator section of heat pipe evaporates. In this case, the main limitation is boiling limitation.

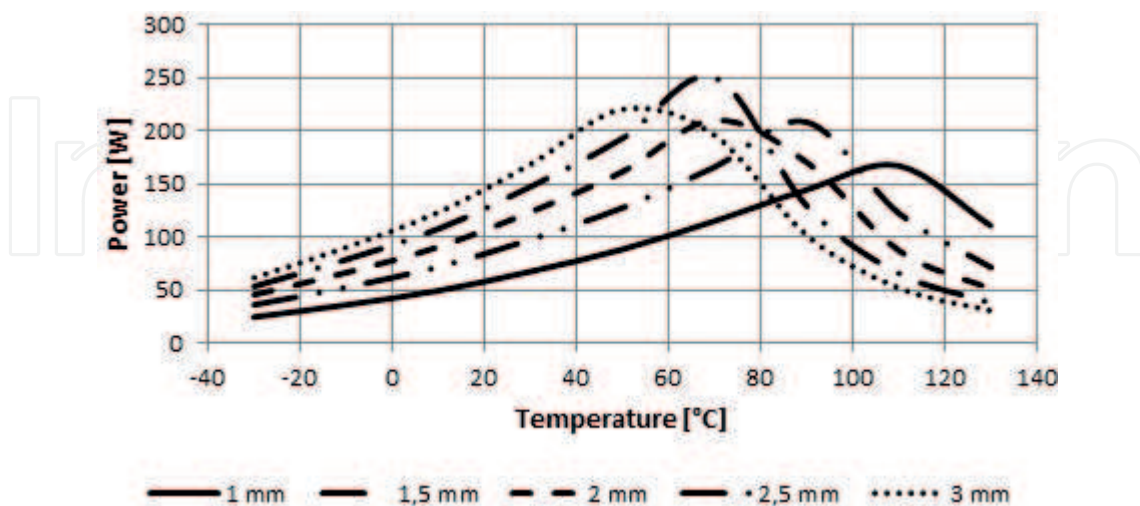


Figure 32. Dependence of heat pipe performance from wick structure width of the sintered wick heat pipe.

6. Conclusion

The experiments performed with the heat pipes in this work give several conclusions about the influence of porous wick structures on their heat transfer ability, where the porosity and pore size play main role. Experiments' influence of manufacturing technology on the wick structure porosity show that the sintering time and temperature of the metal powders are not influencing the wick structure porosity. Other finding of the influence of manufacturing technology on the porous wick structure by the metal powders sintering is that main influencing factors of the wick structure pore size are grain size, sintering temperature, and not so much sintering time.

The experiments' influence of working fluid amount, kind of wick structure and working fluid on heat transfer ability of loop heat pipe show that the optimal amount of the working fluid in LHP is in range 50–60%. In view of influence of the wick structure on the LHP operation, we can conclude that the porosity and pore size of the wick structure have influence on heat transfer ability, when the LHP with porous structure with 50% porosity has better effect on heat removal from IGBT than with 70% and LHP with porous structure with bigger pore size has better effect on heat removal from IGBT than with smaller pore size. Generally, the smallest pore size could cause the low capillary pressure in sintered wick structures against total pressure in whole LHP system. Experimental influence of working fluid on the LHP heat transfer ability shows that the LHP with working fluid acetone better removes heat from the IGBT at lower heat load in range of 100–300 W and LHP with the working fluid water better works at higher heat loads of LHP up to 450 W.

The experiments' influence of the wick structure and working fluid on heat transfer ability of the heat pipe did not show the best one combination of porous wick structure and working fluid. This experiment shows that the heat pipes with porous wick structure are able to transfer heat in range 100–200 W in the horizontal position. It depends on the wick structure parameters and kind of working fluid, because each heat pipe with various combination of these factors is unique due its different properties.

The mathematical calculation of the heat pipe heat transport limitations shows that the critical limitations influencing heat transfer ability of wick heat pipe are entrainment limitation, capillary limitation, and boiling limitation. These limitations depend on thermophysical properties, wick, and heat pipe parameters. The thermophysical properties of each working fluid are stable in temperature range and they cannot change. Changing the dimensions of wick structure is possible to optimize total heat flux transferred by heat pipe, because capillary pressure made in the wick structure depends mainly on the wick structure permeability. When the wick structure is designed, it is necessary to be careful because the increase in pore dimension increases permeability but decreases capillary pressure which manages the working fluid circulation in heat pipe. Therefore, the capillary limitation is the main heat transport limitation in wick heat pipe.

Acknowledgements

This article was created within the frame of projects APVV—15-0778 “Limits of radiative and convective cooling through the phase changes of working fluid in loop thermosyphon” and 042ŽU—4/2016 “Cooling on the basis of physical and chemical processes.”

Author details

Patrik Nemec

Address all correspondence to: patrik.nemec@fstroj.uniza.sk

University of Zilina, Zilina, Slovakia

References

- [1] Gaugler RS. Heat transfer devices. U.S. patent 2,350,348. 1944
- [2] Trefethen L. On the surface tension pumping of liquids or a possible role of the candle-wick in space exploration. In: GE Tech. Int. Ser. No G15-D114. NY: General Electric Co.; 1962
- [3] Grover GM, Cotter TP, Erikson GF. Structures of very high thermal conductivity. *Journal of Applied Physics*. 1964;**35**:1190-1191
- [4] Ochterbeck JM. Heat Pipes, in *Heat Transfer Handbook*. 1st ed. Editors Bejan A, Kraus AD. Hoboken, New Jersey: John Wiley & Sons, Inc.; 2003
- [5] Cernecky J, Koniar J, Brodnianska Z. The effect of heat transfer area roughness on heat transfer enhancement by forced convection. *Journal of Heat Transfer*. April 2014;**136**(4) Article number 4025920
- [6] Swanson LW. In: Kreith F, editor. *Heat Pipe, Heat and Mass Transfer, Mechanical Engineering Handbook*. Boca Raton: CRC Press LLC; 1999
- [7] Reay D, Kew P. *Heat Pipes Theory, Design and Applications*. 5th ed. Oxford, UK: Elsevier; 2006
- [8] Kaya T, Ku J. Thermal operational characteristics of a small-loop heat pipe. *Journal of Thermophysics and Heat Transfer*. 2003;**17**(4):464-470
- [9] Cheung KH, Hoang TT, Ku J, Kaya T. Thermal Performance and Operational Characteristics of Loop Heat Pipe (NRL LHP), SAE Technical Paper, No. 981813, 1998

- [10] Ku J. Operating characteristics of loop heat pipes. In: 29th International Conference on Environmental System, July 12–15, 1999, Denver, Colorado
- [11] Williams RR, Harris DK. Cross-plane and in-plane porous properties measurements of thin metal felts, applications in heat pipes. *Experimental Thermal and Fluid Science*. 2003;**27**:227-235
- [12] Bonnefoy M, Ochterbeck JM. Effective thermal conductivity of saturated sintered nickel loop heat pipe wicks. In: 37th Thermophysics Conference, American Institute of Aeronautics and Astronautics, June 28-July 1, 2004, Portland, Oregon. pp. 1-10
- [13] Holley B, Faghri A. Permeability and effective pore radius measurements for heat pipe and fuel cell applications. *Applied Thermal Engineering*. 2006;**26**:448-462
- [14] Chi SW. *Heat Pipe Theory and Practice: A Sourcebook*. New York: Hemisphere Publishing Corp; 1976
- [15] Čarnogurská M, Příhoda M, Brestovič T, Molínek J, Pyszko R. Determination of permeability and inertial resistance coefficient of filter inserts used in the cleaning of natural gas. *Journal of Mechanical Science and Technology*. 2012;**26**(1):103-111
- [16] Ren C, Wu Q. Heat transfer in loop heat pipes capillary wick, effect effective thermal conductivity. *Journal of Thermophysics and Heat Transfer*. 2007;**21**:134-140
- [17] Khrustalev D, Faghri A. Heat transfer in the inverted meniscus type evaporator at high heat fluxes. *International Journal of Heat and Mass Transfer*. 1995;**38**:3091-3101
- [18] Zhao TS, Liao Q. On capillary-driven flow and phase change heat transfer in a porous structure heated by a finned surface: Measurements and modelling. *International Journal of Heat and Mass Transfer*. 2000;**43**:1141-1155
- [19] Iverson BD, Davis TW, Garimella SV, North MT, Kang SS. Heat and mass transport in heat pipe wick structures. *Journal of Thermophysics and Heat Transfer*. 2007;**21**:392-404
- [20] Launay S, Sartre V, Bonjour J. Parametric analysis of loop heat pipe operation: A literature review. *International Journal of Thermal Sciences*. 2007;**46**:621-636
- [21] Gongming X, Kehang C, Yong Z, Lin C. Reduction of effective thermal conductivity for sintered LHP wicks. *International Journal of Heat and Mass Transfer*. 2010;**53**:2932-2934
- [22] Furukawa M. Model-based method of theoretical design analysis of a loop heat pipe. *Journal of Thermophysics and Heat Transfer*. 2006;**20**:111-121
- [23] Chuang PYA. *An Improved Steady-State Model of Loop Heat Pipes Based on Experimental and Theoretical Analyses [PhD Thesis]*. The Pennsylvania State University; 2003
- [24] Li J, Zou Y, Cheng L, Singh R, Akbarzadeh A. Effect of fabricating parameters on properties of sintered porous wick for loop heat pipe. *Power Technology*. 2010;**204**(2–3):241-248
- [25] Maydanik YF. Loop heat pipes. *Applied Thermal Engineering*. 2005;**25**:635-657

- [26] Patukhov V, Maidanik YF, Vershinin C. Miniature loop heat pipes for electronic cooling. *Applied Thermal Engineering*. 2003;**23**(9):1125-1135
- [27] Reimbrechta EG, Fredel MC, Bazzo E, Pereira FM. Manufacturing and microstructural characterization of sintered nickel wicks for capillary pumps. *Material Research*. 1999; **2**(3):225-229
- [28] Gongming X, Kehang C, Yong Z, Lin C. Development of sintered Ni-Cu wicks for loop heat pipes. *Science in China Series E: Technological Sciences*. 2009;**52**(6):1607-1612
- [29] Huang X, Franchi G. Design and fabrication of hybrid bimodal wick structure for heat pipe application. *Journal Porous Mater*. 2008;**15**:635-664
- [30] Samanta SK, Sharma BB, Das P, Lohar AK. Development of tubular Ni wicks used in LHP for space applications. *Frontiers in Heat Pipes (FHP)*. 2011;**2**. DOI: 043004
- [31] Gernert NJ, Baldassarre GJ, Gottschlich JM. Fine pore loop heat pipe wick structure development, SAE Technical Paper, No. 961319, 1996
- [32] Wu SC, Lo KC, Chen JR, Chung CY, Lin WJ, Su SJ. Effect of sintering temperature curve in wick manufactured for loop heat pipe. *Applied Mechanics and Materials*. 2014;**595**:24-29
- [33] Xin G, Cui K, Zou Y, Cheng L. Development of sintered Ni-Cu wicks for loop heat pipes. *Science in China Series E-Technological Sciences*. 2009;**52**(6):1607-1612
- [34] Orman LJ. Possibility of the application of microstructures in heating and ventilation systems. *Structure and Environment*. 2010;**2**(1):41-45
- [35] Zohuri B. *Heat Pipe Design and Technology: A Practical Approach*. Hillsborough, CA, USA: Galaxy Advanced Engineering; 2011
- [36] Peterson GP. *An Introduction to Heat Pipes: Modelling, Testing and Applications*. Atlanta: Wiley-Interscience; 1994
- [37] Silverstein C. *Design and Technology of Heat Pipes for Cooling and Heat Exchange*. Boca Raton: CRC Press; 1992
- [38] Faghri A. *Heat Pipe Science and Technology*, Washington, DC. Taylor & Francis; 1995
- [39] Chi SW. *Heat Pipe Theory and Practice*. Washington, DC: Hemisphere Publishing; 1976
- [40] Busse CA. Theory of the ultimate transfer of cylindrical heat pipes. *International Journal Heat Mass Transfer*. 1973;**16**:169-186
- [41] Ivanovskii MN, Sorokin VP, Yagodkin IV. *The Physical Properties of Heat Pipes*. Oxford: Clarendon Press; 1982
- [42] Busse CA, Kemme JE. Dry—Out phenomena in gravity— Assist heat pipes with capillary flow. *International Journal Heat Mass Transfer*. 1980;**23**:643-654
- [43] Cotter TP. Heat pipe startup dynamics. *Proceeding of SAE Thermionic Conversion Specialist Conference*, Palo Alto, CA; 1967

- [44] Marcu BD. On the Operation of Heat Pipes, Report 9895-6001-TU-000. Redondo Beach, CA: TRW; 1965
- [45] Dunn PD, Reay DA. Heat Pipes. 3rd ed. New York: Pergamon Press; 1982
- [46] Brennan PJ, Kroliczek EJ. Heat Pipe Design Handbook, NASA Contract Report NAS5-23406, 1979
- [47] Hlavačka V, Polášek F, Štulc P, Zbořil V. Tepelné trubice v elektrotechnice. Praha: STNL - Nakladatelství technické literatury; 1990

IntechOpen

